

55752-63-1; **16a**, 75526-82-8; **16b**, 97938-47-1; **16c**, 102860-35-5; **16d**, 114505-84-9; **16e**, 76426-55-6; **16f**, 114492-39-6; **16g**, 114505-85-0; **10h**, 114505-86-1; **16i**, 79815-55-7; **16j**, 114505-87-2; **16k**, 114505-88-3; **16l**, 114492-31-8; **17**, 23876-79-1; **19a**, 271-44-3; **19b**, 5401-94-5; **19c**, 95-14-7; **20a**, 114505-89-4; **20b**, 114505-90-7; **20c**, 114505-91-8; **21a**, 2039-06-7; **21b**, 3357-42-4; **22a**, 114505-92-9; **22b**, 114505-93-0; **23a**, 10199-63-0; **23b**, 36140-84-8; **3c**, 3C140-83-7; **24a**, 76434-58-7; **24b**, 114505-94-1; **24c**, 114505-95-2; **24d**, 91994-38-6; **24e**, 91994-39-7; **24f**, 114505-96-3; **25a**, 75-44-5; **25b**,

463-71-8; **25c**, 1886-67-5; **25d**, 10472-00-1; **26a**, 616-47-7; **28b**, 7164-98-9; **27a**, 91994-35-3; **27b**, 114492-26-1; **27c**, 114505-26-9; **28** (R = CH<sub>3</sub>, R' = C<sub>6</sub>H<sub>5</sub>), 114505-97-4; **29**, 1632-83-3; **30a**, 114492-42-1; **30b**, 114492-27-2; **30c**, 114492-43-2; **31b**, 91994-41-1; **32**, 13423-60-4; **34**, 114532-37-5; **35**, 16227-12-6; **37**, 114505-98-5; **38**, 32137-73-8; **39**, 114505-99-6; **40**, 25705-34-4; **41**, 114506-00-2; **42**, 78948-36-4; **43**, 114506-01-3; (C<sub>2</sub>H<sub>5</sub>O)<sub>2</sub>CHCHO, 6367-37-9; CHCl(COCH<sub>3</sub>)<sub>2</sub>, 1694-29-7; 2-bromopyridine, 109-04-6; 1,3-bis-(3,5-dimethylpyrazol-1-yl)-1,3-propanedione, 31705-94-9.

## Cross-Conjugated and Pseudo-Cross-Conjugated Mesomeric Betaines. 2. Structure and Reactivity<sup>†</sup>

Kevin T. Potts,\* Peter M. Murphy, Mark R. DeLuca, and William R. Kuehnling<sup>1</sup>

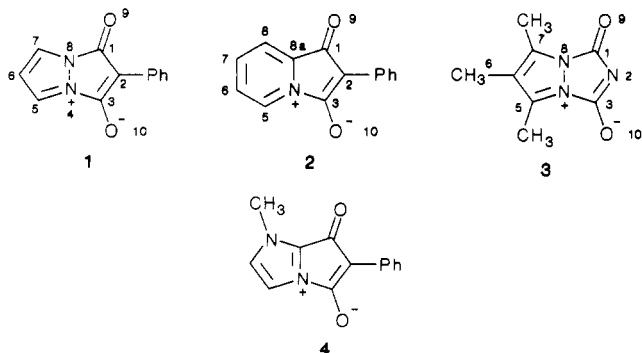
Department of Chemistry, Rensselaer Polytechnic Institute, Troy, New York 12181

Received October 26, 1987

A theoretical and experimental study of cross-conjugated (CCMB) and pseudo-cross-conjugated (PCCMB) mesomeric betaines shows that they are best represented as containing distinct cationic and anionic segments which comprise a common  $\pi$ -electron system. The PCCMB differ from the CCMB in that they all contain a 2-oxyallyl cation 1,3-dipole. The behavior of these betaines under electrophilic and nucleophilic reaction conditions has been established.

In the preceding paper, synthetic methods leading to a variety of cross-conjugated (CCMB) and pseudo-cross-conjugated (PCCMB) mesomeric betaines have been described. We now report our theoretical and physical organic chemical studies which provide support for the classification of these cross-conjugated mesomeric betaines, establish the reactivity of these betaines under a variety of conditions, and by defining structural parameters, enable predictions to be made regarding further development of this concept.

**X-ray Data.** A single-crystal X-ray study of anhydro-1-hydroxy-3-oxo-2-phenylpyrazolo[1,2-*a*]pyrazolium hydroxide (**1**), a CCMB, showed<sup>2</sup> that the molecule is pseudoplanar with a 2-fold axis of symmetry and that the 2-phenyl substituent is twisted 7.3° out of the plane. Of particular interest is the N(8)–C(1) bond length of 1.49 Å, a "union bond" which approximates a normal N–C single bond, while the C(1)–O(9) bond length is 1.22 Å, consistent with a normal C=O bond length. These data are in agreement with negative charge delocalization over the  $\beta$ -diketone enolate and the phenyl ring and the positive charge being delocalized over the pyrazolium ring.



The X-ray structure of a PCCMB, anhydro-1-hydroxy-3-oxo-2-phenylpyrazolo[1,5-*a*]pyridinium hydroxide (**2**), was similar in many respect to that of **1** above. In particular, the C(8a)–C(1) bond length was 1.51 Å and the N(4)–C(3) bond length was 1.52 Å, again signifying no appreciable  $\pi$ -overlap between the pyridinium ring and the  $\beta$ -diketone system. The 2-phenyl substituent was twisted 13.0° from the plane of the bicyclic system. The C(1)–O(9) bond length of 1.24 Å approximates that of a normal carbonyl group. The data for **2** shows a pseudo 2-fold axis of symmetry, resulting in some disorder in the crystal. The X-ray data for structure **2** is shown in Figure 1, and further details are provided in the supplementary material.

It is particularly interesting that the X-ray data of the CCMB **3**, anhydro-1-hydroxy-3-oxo-5,6,7-trimethylpyrazolo[1,2-*a*]-1,2,4-triazolium hydroxide, shows<sup>3</sup> remarkable consistency with the bond lengths of **1** and **2**. For example, the N(8)–C(1) bond length is 1.49 Å and the C(1)–O(9) bond length is 1.18 Å. The consistency in the "union bonds" approximating single bonds is also observed in the X-ray data of several six-membered CCMB containing a pyrimidine<sup>4</sup> and a 1,3-oxazine<sup>5</sup> nucleus.

**Dipole Moments.** The hypothesis advanced to rationalize the structures of CCMB and PCCMB requires a high degree of charge separation which would be reflected in the dipole moment. Figure 2 shows the experimental<sup>6</sup>

(1) Abstracted from the Ph.D. theses of W. R. K. (1984) and P. M. M. (1987), Rensselaer Polytechnic Institute; acknowledgement is made to the donors of the Petroleum Research Fund, administered by the ACS, for partial support of this work (PRF Grant 13306-AC4). Part of this work appeared in a Preliminary Communication. Potts, K. T.; Murphy, P. M. *J. Chem. Soc., Chem. Comm.* 1986, 144.

(2) Raston, C. L.; White, A. H. *Aust. J. Chem.* 1984, 37, 2577.

(3) Friedrichsen, W.; Bottcher, A.; Debaerdemeker, T. *Heterocycles* 1983, 20, 23.

(4) Kratky, Ch.; Kappe, T. *J. Heterocycl. Chem.* 1981, 18, 881.

(5) Debaerdemeker, T.; Friedrichsen, W. *Z. Naturforsch., B: Anorg. Chem., Org. Chem.* 1982, 37B, 217.

(6) Guggenheim, E. A. *Trans. Faraday Soc.* 1951, 47, 573. Smith, J. W. *Trans. Faraday Soc.* 1950, 46, 394.

<sup>†</sup> Dedicated to Prof. E. C. Taylor on the occasion of his 65th birthday.

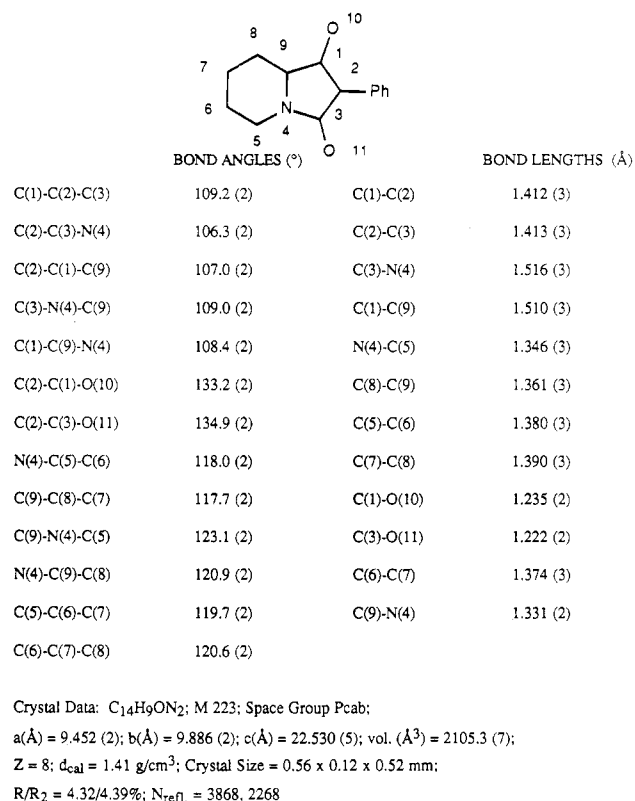


**Figure 1.** X-ray geometry of anhydro-1-hydroxy-3-oxo-2-phenylpyrrolo[1,2-a]pyridinium hydroxide.

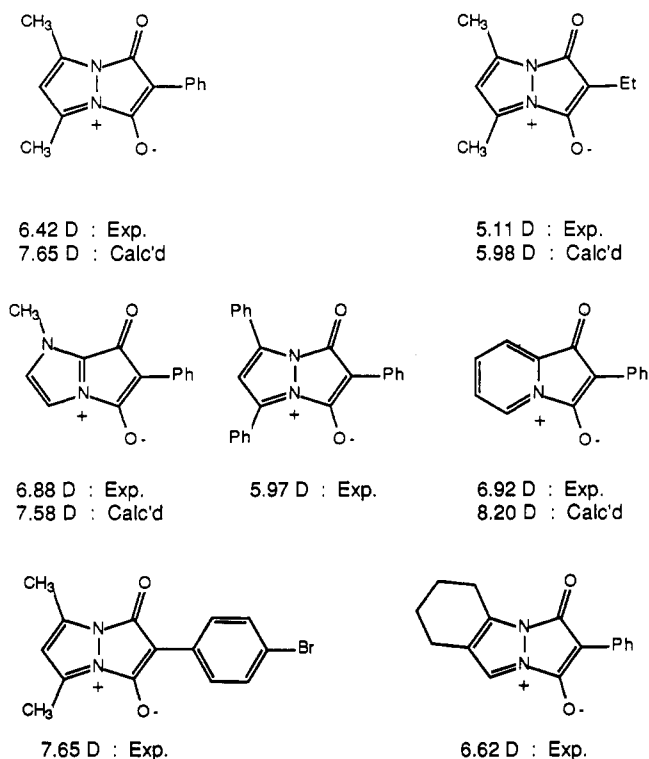


**Figure 2.** Dipole moments of mesomeric betaines obtained from MINDO/3 calculations.

dipole moments of a number of CCMB and PCCMB which vary from 5.11 to 7.65 D, the direction of the moment being from the cationic to the anionic portion of the molecule. For a neutral organic molecule, these values in Figure 2 represent large dipole moments; similar values have been reported for the neutral mesoionic sydnone systems (5.0–7.3 D)<sup>7</sup> and for 4-nitroanisole<sup>8</sup> (5.26 D).

**Table I.** Comparison of Experimental<sup>2</sup> and Calculated Geometry of Anhydro-1-hydroxy-3-oxo-2-phenylpyrrolo[1,2-a]pyrazolium Hydroxide (1)

	X-ray anal.: bond length (Å)	MINDO/3 minimized
C(1)–C(2)	1.41	1.41
C(1)–O(9)	1.22	1.21
C(1)–N(8)	1.49	1.48
N(4)–N(8)	1.34	1.35
N(4)–C(5)	1.34	1.36
C(5)–C(6)	1.38	1.41
	X-ray anal.: bond angle (deg)	MINDO/3 minimized
O(9)–C(1)–C(2)	137	141
O(9)–C(1)–N(8)	118	114
N(8)–C(1)–C(2)	105	106
C(1)–C(2)–C(3)	111	110
C(1)–N(8)–N(4)	109	110
N(4)–N(8)–C(7)	109	109
C(1)–N(8)–C(7)	142	142
N(4)–C(5)–C(6)	108	107
C(5)–C(6)–C(7)	107	107

The presence of the 2-phenyl substituent in both CCMB and PCCMB results in an increase in the dipole moment of approximately 1.3 D, in keeping with the extended conjugation present in the anionic portion of the molecule. The introduction of a 4-bromophenyl substituent into the 2-position of the pyrrolo[1,2-a]pyrazolium hydroxide system significantly increases the dipole moment and allows one to determine the direction of the moment.

**Electrochemistry.** Cyclic voltammetry of CCMB and a PCCMB has been reported<sup>9</sup> and shows 1 and aryl substituted derivatives (Br, NO<sub>2</sub>) to have reduction potentials in the range –0.96 to –1.34 V. The corresponding 5,7-dimethyl derivative has  $E_p = -1.42$  V, and on replacement of the 2-phenyl substituent with an ethyl group, the  $E_p = -1.55$  V. These reduction potentials were found to fit the modified Hammett equation. Anhydro-1-hydroxy-7-methyl-3-oxo-2-phenylpyrrolo[1,2-a]imidazolium hydroxide (4), a PCCMB, underwent more ready reduction (–0.88 V).

**Theoretical Methods.** In our study several MO methods were used to evaluate theoretically CCMB and PCCMB. MINDO/3, STO-3G, and 3-21G and Hückel procedures were used. Table I illustrates the excellent agreement between MINDO/3 minimized molecular geometries<sup>10</sup> (bond lengths, bond angles) and those obtained<sup>2</sup> from single-crystal X-ray data for the CCMB 1. The average deviation is less than 2% except for the O(9)–C(1)–C(2) bond angle, where the deviation was <4%. Table II shows similar data for the PCCMB 2, where the average deviation is less than 2% except for the “union bonds” joining the pyridinium moiety to the β-diketone system, where the deviation was slightly less than 4%. The similar

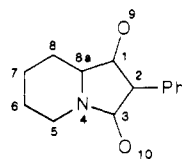
(7) Clapp, L. B. In *Comprehensive Heterocyclic Chemistry*; Potts, K. T., Ed.; Pergamon: Oxford, 1984; Vol. 6, p 368.

(8) Nelson, R. D.; Lide, D. R.; Maryott, A. A. In *National Reference Data Series—National Bureau of Standards*; NSRDS-NBS 10.

(9) Ames, J. R.; Potts, K. T.; Ryan, M. D.; Kovacic, P. *Life Sci.* 1986, 39, 1085.

(10) Dewar, M. J. S. *Science (Washington, D.C.)* 1975, 187, 1037 and references therein.

**Table II. Comparison of Experimental and Calculated Geometry of Anhydro-1-hydroxy-3-oxo-2-phenylpyrrolo[1,2-*a*]pyridinium Hydroxide (2)**



	X-ray anal.: bond length (Å)	MINDO/3 minimized
C(1)–C(2)	1.41	1.45
C(2)–C(3)	1.41	1.43
C(3)–N(4)	1.52	1.54
C(1)–C(8a)	1.51	1.55
N(4)–C(5)	1.35	1.38
C(8)–C(8a)	1.36	1.40
C(5)–C(6)	1.38	1.38
C(7)–C(8)	1.39	1.41
C(1)–O(9)	1.24	1.21
C(3)–O(10)	1.22	1.20
C(6)–C(7)	1.37	1.41
C(8a)–N(4)	1.33	1.33

	X-ray anal.: bond angle (deg)	MINDO/3 minimized
C(1)–C(2)–C(3)	109	108
C(2)–C(3)–N(4)	106	106
C(2)–C(1)–C(8a)	107	106
C(3)–N(4)–C(8a)	109	109
C(1)–C(8a)–N(4)	108	109
C(2)–C(1)–O(9)	133	135
C(2)–C(3)–O(10)	135	136
N(4)–C(5)–C(6)	118	120
C(8a)–C(8)–C(7)	118	119
C(8a)–N(4)–C(5)	123	122
N(4)–C(8a)–C(8)	121	122
C(5)–C(6)–C(7)	120	120
C(6)–C(7)–C(8)	121	119

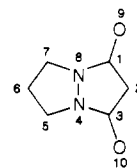
values for both bond lengths and bond angles lend support to the contention that MINDO/3 calculations reliably reflect the observed physical and chemical properties of CCMB and PCCMB.

Charge densities and HOMO/LUMO coefficients were determined by several methods, and comparative results are shown in Table III and IV. The results in Table III clearly show the high degree of negative charge developed on the exocyclic oxygen atoms and on C<sub>2</sub> of the  $\beta$ -diketone anion system described above. Qualitatively, the agreement between the charge densities obtained via the different methods is quite good. The largest deviation occurs with the two ab initio methods and may be attributed to our inability to minimize cost-effectively in computer time with such a large molecule. The presence of the pyrazolium ion is also shown by these charge densities, which are in agreement with published data for the pyrazolium system.<sup>11</sup>

Figure 2 shows experimental and calculated dipole moments for several CCMB and PCCMB. Taking into account the difference between solution measurements and theoretical calculations involving gas-phase conditions, the dipole moment data obtained from MINDO/3 calculations clearly show the large charge separation and are in good agreement with the experimental values.

In Table IV, which shows HOMO and LUMO profiles for the parent anhydro-1-hydroxy-3-oxopyrrolo[1,2-*a*]pyrazolium hydroxide (5), the good agreement between the various methods used is readily apparent. They clearly

**Table III. Calculated Net Atomic Charge Densities for Anhydro-1-hydroxy-3-oxopyrazolo[1,2-*a*]pyrazolium Hydroxide**



A. $\pi$ -Electrons Only					
atom no.	Hückel	$\omega$ -Hückel	MINDO/3	STO-3G	3-21G
C <sub>1</sub> /C <sub>3</sub>	+0.2	+0.1	+0.4	0.0	+0.2
C <sub>2</sub>	-0.3	-0.2	-0.5	-0.4	-0.4
N <sub>4</sub> /N <sub>8</sub>	+0.4	+0.4	+0.5	+0.5	+0.5
C <sub>5</sub> /C <sub>7</sub>	+0.2	+0.2	+0.1	0.0	+0.1
C <sub>6</sub>	-0.1	0.0	-0.2	-0.1	-0.1
O <sub>9</sub> /O <sub>10</sub>	-0.7	-0.5	-0.6	-0.5	-0.5
Net Charge Separation: Cationic–Anionic					
	1.1	1.1	1.1	1.0	1.0

B. $\sigma$ - and $\pi$ -Electrons			
atom no.	MINDO/3	STO-3G	3-21G
C <sub>1</sub> /C <sub>3</sub>	+0.7	-0.3	+0.9
C <sub>2</sub>	-0.5	-0.1	-0.5
N <sub>4</sub> /N <sub>8</sub>	0.0	+0.3	-0.7
C <sub>5</sub> /C <sub>7</sub>	+0.1	+0.1	+0.3
C <sub>6</sub>	-0.2	-0.1	-0.5
O <sub>9</sub> /O <sub>10</sub>	-0.5	-0.3	-0.6
Net Charge Separation: Cationic–Anionic			
	0.2	0.3	0.2
Calculated Dipole Moments (D)			
	4.7	6.0	7.3

show that the HOMO is associated with the  $\beta$ -diketone anion portion of the molecule and that the node of the MO passes through the pyrazole cation. This substantiates the concept of union through nodal positions of the MO of an alternate hydrocarbon anion to form the CCMB and PCCMB. The LUMO profile shows charge distribution throughout the molecule.

These theoretical studies above provide a guide for our chemical and spectroscopic characterization described below.

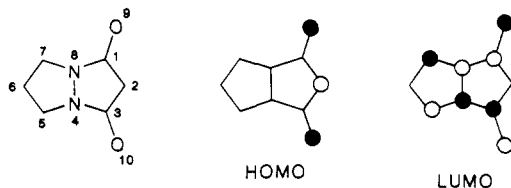
**Spectroscopic Methods.** <sup>1</sup>H and <sup>13</sup>C NMR data for CCMB and PCCMB have been extremely important for structural proof and also for providing evidence of charge distribution. In 5 the C<sub>2</sub>-H was observed at  $\delta$  4.22, the C<sub>5</sub>/C<sub>7</sub>-H at  $\delta$  7.99, and the C<sub>6</sub>-H at  $\delta$  6.72. In the corresponding 5,7-dimethyl compound, only slight changes were observed for the C<sub>2</sub>-H at  $\delta$  4.16 and the C<sub>6</sub>-H at  $\delta$  6.16. Introduction of bromine or iodine into the 2-position of the anhydro-5,7-dimethyl-1-hydroxy-3-oxopyrazolo[1,2-*a*]pyrazolium hydroxide likewise had a very small effect on the C<sub>6</sub>-H ( $\delta$  6.21 for Br,  $\delta$  6.15 for I) chemical shifts and on the methyl chemical shifts which were at  $\delta$  2.65 for both the bromo- and iodo-substituted compounds.

The chemical shifts of C<sub>2</sub>-H in 5 and its 5,7-dimethyl derivative are similar to the chemical shifts of analogous protons in the enolate salts of diethyl malonate<sup>12</sup> ( $\delta$  3.77), ethyl acetoacetate<sup>12</sup> ( $\delta$  4.36), and acetylacetone<sup>12</sup> ( $\delta$  4.93). This deshielding of the C<sub>2</sub>-H is indicative of the high charge density at the C<sub>2</sub> position predicted by our theoretical calculations. Conversely, the chemical shifts of the C<sub>5</sub>/C<sub>7</sub>-H and C<sub>6</sub>-H are analogous to the corresponding protons in the pyrazolium ion which occur at C<sub>3</sub>/C<sub>5</sub>-H at  $\delta$  8.57 and C<sub>4</sub>-H at  $\delta$  8.87.

(11) Vaughan, J. D.; O'Donnell, M. *Tetrahedron Lett.* 1968, 3727.

(12) Howden, M. E. H.; Taylor, M. *Tetrahedron Lett.* 1975, 1979.

Table IV. HOMO and LUMO Profiles for Anhydro-1-hydroxy-3-oxopyrazolo[1,2-a]pyrazolium Hydroxide



atom no.	HOMO coefficients				
	Hückel	$\omega$ -Hückel	MINDO/3	STO-3G	3-21G
1	-0.2	-0.2	-0.1	-0.1	-0.1
2	-0.7	-0.6	-0.8	-0.7	-0.8
3	-0.2	-0.2	-0.1	-0.1	+0.1
4	+0.1	0.0	+0.2	0.0	+0.1
5	0.0	0.0	-0.1	0.0	0.0
6	-0.1	0.0	-0.2	0.0	-0.1
7	0.0	0.0	-0.1	0.0	0.0
8	+0.1	0.0	+0.2	0.0	+0.1
9	+0.5	+0.6	+0.3	+0.5	+0.4
10	+0.5	+0.6	+0.3	+0.5	+0.4

Energy					
$\alpha + 0.59\beta$		$\alpha + 0.13\beta$	-0.89 eV	-0.19 eV	-0.31 eV
atom no.	LUMO coefficients				
	Hückel	$\omega$ -Hückel	MINDO/3	STO-3G	3-21G
1	-0.4	-0.2	-0.3	-0.2	-0.2
2	0.0	0.0	0.0	0.0	0.0
3	+0.4	+0.2	+0.3	+0.2	+0.2
4	+0.2	+0.3	+0.4	+0.4	+0.4
5	-0.5	-0.5	-0.5	-0.5	-0.5
6	0.0	0.0	0.0	0.0	0.0
7	+0.5	+0.5	+0.5	+0.5	+0.5
8	-0.2	-0.3	-0.4	-0.4	-0.4
9	+0.3	+0.3	+0.2	+0.3	+0.3
10	-0.3	-0.3	-0.2	-0.3	-0.3

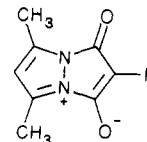
  

Energy					
$\alpha - 0.37\beta$		$\alpha - 0.31\beta$	-0.03 eV	+0.14 eV	-0.04 eV

In the PCCMB series, our inability to prepare representatives unsubstituted at  $C_2$  precludes obtaining direct  $^1\text{H}$  NMR evidence of charge distribution over the  $\beta$ -diketone moiety as described above. However, the chemical shifts of the protons in the 2-phenyl substituent show that the substituent is attached to a center bearing a high charge density. Thus, in the PCCMB 2, the chemical shift of the para hydrogen atom was  $\delta$  7.19, that of the meta hydrogen atoms was  $\delta$  8.28, and that of the ortho hydrogen atoms was  $\delta$  7.20, with the usual aromatic coupling being observed. The decreased shielding of the ortho and para protons reflects an increase in the charge densities at those positions, attributable to delocalization of the  $\beta$ -diketone's negative charge over the aromatic ring, which was also indicated by the X-ray data. A similar trend was observed for all PCCMB as well as CCMB containing 2-aryl substituents.

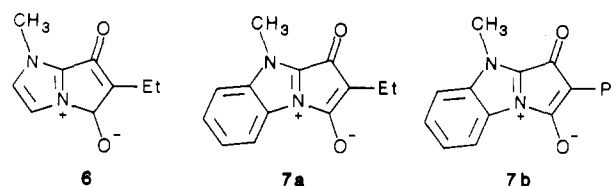
In the cationic portion of the PCCMB 2, the  $C_5$ -H,  $C_6$ -H,  $C_7$ -H, and  $C_8$ -H were observed at  $\delta$  8.71, 7.83, 8.42, and 7.90, respectively. These chemical shifts are consistent with the chemical shifts of analogous protons in the pyridinium ion.<sup>13a</sup> Similarly in 4 the  $C_5$ -H and  $C_6$ -H were at  $\delta$  7.22 and 6.88, respectively. The corresponding protons in the 1-methylimidazolium ion are at  $\delta$  7.53 ( $C_4$ -H) and 7.65 ( $C_5$ -H).

Table V.  $^{13}\text{C}$  NMR Data for 2-Substituted Anhydro-5,7-dimethyl-1-hydroxy-3-oxopyrazolo[1,2-a]pyrazolium Hydroxides



R	$^{13}\text{C}$ NMR chemical shifts (ppm)				
	$C_1/C_3$	$C_2$	$C_5/C_7$	$C_6$	$\text{CH}_3$
H	161.4	68.9	111.4	142.7	11.0
Br	156.6	59.7	111.4	144.2	11.3
Et	161.2	82.3	110.9	142.5	11.0
Ph	159.2	82.0	111.7	143.2	11.0
CN	157.5	112.2	113.4	145.5	11.5
$\text{CH}_2\text{CH}_2\text{Cl}$	161.5	81.6	111.2	143.0	11.0
$p\text{-BrC}_6\text{H}_4$	159.0	81.7	111.8	143.3	11.7
$p\text{-CH}_3\text{OC}_6\text{H}_4$	159.3	81.9	111.5	143.0	11.0
$2,4\text{-(NO}_2)_2\text{C}_6\text{H}_3$	157.4	80.9	112.6	144.1	11.4
$o\text{-NO}_2\text{C}_6\text{H}_4$	158.2	80.7	112.0	144.0	11.2
$p\text{-NH}_2\text{C}_6\text{H}_4$	158.9	81.3	112.2	143.5	10.6

Table VI.  $^{13}\text{C}$  Chemical Shifts (ppm,  $\text{CDCl}_3$ ) for Carbon Atoms in the  $\beta$ -Diketone Segment of Several PCCMB



compd no.	$C_1$	$C_2$	$C_3$
2	164.2	89.2	178.2
4	161.6	94.7	169.0
6	163.2	96.2	170.3
7a	165.0	100.2	168.4
7b	163.6	97.3	167.5

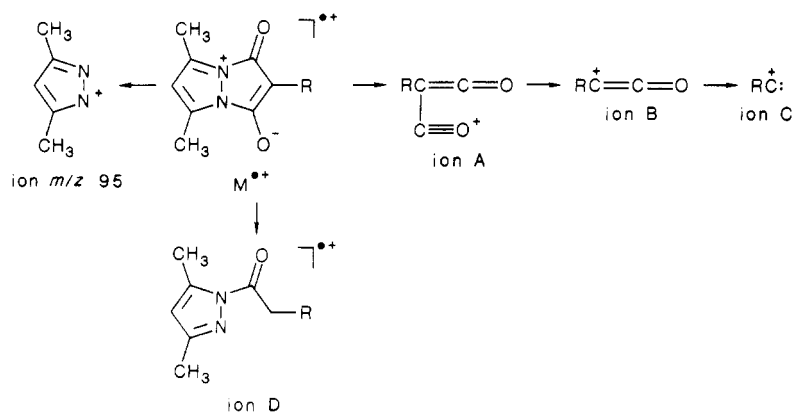
The  $^{13}\text{C}$  NMR data are noticeably consistent with the  $^1\text{H}$  chemical shifts of the attached protons in both CCMB and PCCMB.  $^{13}\text{C}$  chemical shifts for representative pyrazolium CCMB are shown in Table V, and particularly noteworthy among these data are the chemical shifts of  $C_2$ . With no substituent at  $C_2$ , the chemical shift was 68.9 ppm, indicative of high deshielding of the  $\text{sp}^2$  carbon atom. Introduction of an ethyl group at this position influenced this deshielding appreciably, resulting in a shift to 82.3 ppm ( $\Delta = 13.4$  ppm). A similar shift was observed with 2-chloroethyl, phenyl, and substituted phenyl substituents, the range being from 80.7 to 82.0 ppm. A 2-bromo substituent resulted in further deshielding, with the  $C_2$  chemical shift now at 59.7 ppm. Conversely, introduction of a cyano group resulted in shielding of the  $C_2$  carbon atom and a subsequent chemical shift to 112.2 ppm.

The chemical shifts of the  $C_1$  and  $C_3$  carbonyl carbon atoms fall in the range 156.6–161.5 ppm, upfield from the normal ketone carbonyl absorption region of 175–225 ppm. As the X-ray data has excluded any significant amide conjugation, this high-field shift indicates delocalization of the negative charge over the  $\beta$ -diketone system. The influence of substituents on other ring carbon atoms is apparent from Table V.

In PCCMB (Table VI), although  $C_2$  is appreciably deshielded relative to a normal  $\text{sp}^2$  carbon atom, the deshielding is not as great as that observed in the CCMB above. We attribute this more to differences in the cationic portions of the bicyclic system than to differences in charge separation, for the PCCMB 2 and 4 had larger dipole moments (6.92 and 6.88 D) than the analogously substi-

(13) (a) Yoneda, S.; Sugimoto, T.; Yoshida, Z. *Tetrahedron* 1973, 29, 2009. (b) Schwartz, H. M.; MacCoss, M.; Danyluk, S. S. *Magn. Reson. Chem.* 1985, 23, 885. Schwartz, H. M.; MacCoss, M.; Danyluk, S. S. *J. Am. Chem. Soc.* 1983, 105, 5901. Cheng, C. P.; Lin, S. C.; Shaw, G.-S. *J. Magn. Reson.* 1986, 69, 58.

Table VII. Mass Spectral Fragmentation Patterns of CCMB



R in $M^{+\bullet}$	$M^{+\bullet}$ $m/z^a$	ion $m/z$ 95	ion A $m/z$	ion B $m/z$	ion C $m/z$	ion D $m/z$
H	164 (45)	(100)	64 (24)	—	—	—
Br	$^{79}\text{Br}$ 244 (100) $^{81}\text{Br}$ 246 (99)	(63)	$^{79}\text{Br}$ 149 (47) $^{81}\text{Br}$ 147 (46)	$^{79}\text{Br}$ 121 (11) $^{81}\text{Br}$ 123 (11)	$^{79}\text{Br}$ 93 (16) $^{81}\text{Br}$ 91 (16)	$^{79}\text{Br}$ 216 (19) $^{81}\text{Br}$ 218 (19)
I	290 (100)	(33)	195 (14)	167 (8)	139 (15)	262 (6)
Ph	240 (100)	(84)	145 (21)	117 (13)	89 (45)	212 (10)
CN	189 (100)	(6)	94 (35)	66 (16)	38 (13)	161 (19)
Et	192 (30)	(8)	97 (12)	69 (11)	—	158 (<2)

<sup>a</sup> Values in parentheses are relative intensity.

tuted CCMB. In this series, two distinct carbonyl carbon resonances were observed, one upfield in the 161–165 ppm region and one downfield from 168–178 ppm. At first sight it is difficult to assign a particular chemical shift to either the  $C_1$  or the  $C_3$  carbon atom. Carbon–carbon connectivity NMR experiments failed to differentiate between the individual carbon atoms of the two carbonyl groups due to the insensitivity of these methods, and our assignment of  $C_1$  and  $C_3$  chemical shifts is based upon the charge densities of the two carbonyl carbon atoms determined by various MO methods. The more electropositive carbon atom is the one bound to the nitrogen atom of the cationic segment and was assigned to the further downfield carbon signal.

The  $^{17}\text{O}$  NMR spectra of anhydro-5,7-dimethyl-1-hydroxy-3-oxopyrazolo[1,2-*a*]pyrazolium hydroxide and the corresponding 2-phenyl compound each showed one signal at 290.5 and 307.6 ppm, respectively. These chemical shifts of the oxygen atoms of pyrazolium CCMB indicate double-bond character in the carbonyl group,<sup>13b</sup> consistent with substantial delocalization of the negative charge through  $C_2$ .

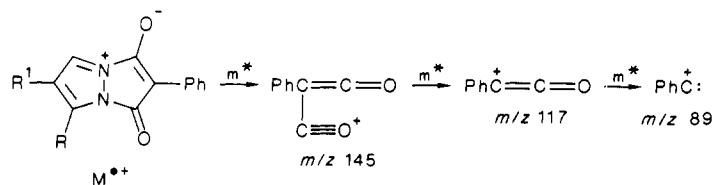
**Infrared Spectra.** The CCMB studied showed an intense carbonyl absorption in the range 1670–1715  $\text{cm}^{-1}$  and a shoulder on this absorption at 1725–1780  $\text{cm}^{-1}$ . In contrast the PCCMB showed two distinct, intense carbonyl absorptions at 1600–1635 and 1700–1740  $\text{cm}^{-1}$ . The absorption in the 1700–1740- $\text{cm}^{-1}$  range in the latter is considered to be that carbonyl group adjacent to the nitrogen atom at the ring junction and reinforces the contention that there is no lone-pair resonance contribution from the nitrogen atom to the carbonyl group. The inductive effect of the nitrogen atom does cause the carbonyl group absorption to shift to higher energy, and these absorptions are supportive of the cross-conjugated concept. The delocalization of the anionic charge at  $C_2$  results in a lower energy carbonyl absorption for both of the carbonyl groups.

**Mass Spectral Studies.** The majority of the CCMB and PCCMB studied showed intense molecular ions in their electron-impact mass spectra. Fragmentation of the molecular ions consistently follows two pathways, the first being (1) cleavage of the “union bonds” to give rise to two

fragments, the cationic heterocycle and the carbonylketene cation. These may be generated in two ways: (a) fragmentation of the molecular ion to give the cationic heterocycle and the neutral carbonylketene fragment, which is then ionized; and (b) generation of the carbonylketene cation and a neutral heterocyclic fragment, which is then ionized. Of course both processes may be operating simultaneously where the influence of substituents plays a predominant role. The data shown in Table VII are not sufficiently definitive to determine which process is favored. (2) Loss of CO from the molecular ion is the second fragmentation pathway generating a radical cation. Daughter ions consistent with loss of the heterocycle from this radical cation are also observed.

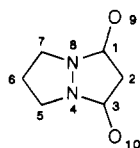
An analysis of the metastable ions ( $m^*$ ) in the electron-impact mass spectra of several pyrazolium CCMB provides evidence for the dominant pathway in their fragmentation. The data in Table VIII indicate that the molecular ion fragments into a neutral pyrazole radical and a phenylcarbonylketene cation. The loss of carbon monoxide from the phenylcarbonylketene cation gives rise to the phenylketene cation and the phenylcarbene cation. These fragmentation patterns are consistent to varying degrees in all CCMB and PCCMB, and they may be considered diagnostic for CCMB and PCCMB containing a 1,3-diketone moiety (Table VII).

**UV-Visible Spectra.** The HOMO and LUMO of the CCMB and PCCMB suggest that, upon electronic excitation from the HOMO to the LUMO, considerable electron density is shifted from the  $\beta$ -diketone enolate moiety to the pyrazolium ion. Table IX shows both the ground-state and excited-state  $\pi$ -charge densities calculated for 5. Comparison of the total  $\pi$ -charge density on the right- and left-hand sides of the molecule in the ground state was offered previously as evidence for the predicted charge separation in 5 and related systems. A similar comparison of the total excited-state  $\pi$ -charges on these two moieties consistently predicts a transfer of considerable charge density from the  $\beta$ -diketo enolate to the pyrazolium ion upon excitation of one electron from the HOMO to the LUMO. The actual amount of charge transferred is dependent upon the calculation method used, varying from

**Table VIII. Principal Metastable Ions Observed in the Fragmentation of Substituted Anhydro-1-hydroxy-3-oxo-2-phenylpyrazolo[1,2-a]pyrazolium Hydroxides**

substituents in M <sup>2+</sup>	M <sup>2+</sup> <sup>a</sup>	transition	m* calcd	m* obsd	fragment expelled
R = R <sup>1</sup> = H	212 (100)	212→145	99.2	97.8 (39)	C <sub>3</sub> H <sub>3</sub> N <sub>2</sub>
		145→117	94.4	94.4 (29)	CO
		117→89	67.7	67.7 (88)	CO
R = CH <sub>3</sub> , R <sup>1</sup> = H	226 (100)	226→145	—	—	—
		145→117	94.4	94.4 (23)	CO
		117→89	67.7	67.7 (63)	CO
R = CH <sub>3</sub> , R <sup>1</sup> = NO <sub>2</sub>	271 (88)	271→145	77.6	77.6 (75)	C <sub>4</sub> H <sub>4</sub> N <sub>3</sub> O <sub>2</sub>
		145→117	94.4	94.4 (34)	CO
		117→89	67.7	67.7 (100)	CO
R = R <sup>1</sup> = C <sub>4</sub> H <sub>4</sub> <sup>b</sup>	262 (53)	262→145	80.2	80.2 (45)	C <sub>7</sub> H <sub>5</sub> N <sub>2</sub>
		145→117	94.4	94.4 (25)	CO
		117→89	67.7	67.7 (100)	CO
R = R <sup>1</sup> = C <sub>4</sub> H <sub>3</sub> NO <sub>2</sub> <sup>c</sup>	307 (64)	307→145	68.5	68.5 (50)	C <sub>7</sub> H <sub>4</sub> N <sub>3</sub> O <sub>2</sub>
		145→117	94.4	94.4 (35)	CO
		117→89	67.7	67.7 (100)	CO

<sup>a</sup> Values in parentheses are relative intensity. <sup>b</sup> Derived from indazole. <sup>c</sup> Derived from 5-nitroindazole.

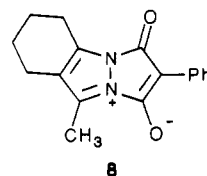
**Table IX. Calculated Atomic Ground State and Excited State  $\pi$ -Charge Densities for Anhydro-1-hydroxy-3-oxopyrazolo[1,2-a]pyrazolium Hydroxide**

atom no.	ground-state (excited-state) $\pi$ -charge densities			
	Hückel	MINDO/3	STO-3G	3-21G
C <sub>1</sub> /C <sub>3</sub>	0.9 (1.0)	0.6 (0.7)	1.0 (1.0)	0.8 (0.9)
C <sub>2</sub>	1.2 (0.8)	1.5 (0.9)	1.4 (0.9)	1.4 (0.9)
N <sub>4</sub> /N <sub>8</sub>	1.6 (1.7)	1.5 (1.6)	1.4 (1.6)	1.5 (1.7)
C <sub>5</sub> /C <sub>7</sub>	0.8 (1.1)	0.9 (1.1)	1.0 (1.2)	0.9 (1.1)
C <sub>6</sub>	1.0 (1.0)	1.2 (1.1)	1.1 (1.1)	1.1 (1.1)
O <sub>9</sub> /O <sub>10</sub>	1.5 (1.3)	1.6 (1.6)	1.3 (1.2)	1.5 (1.3)
right side (C <sub>1</sub> , C <sub>2</sub> , C <sub>3</sub> , O <sub>9</sub> , O <sub>10</sub> )	6.0 (5.3)	6.1 (5.5)	6.0 (5.3)	6.1 (5.3)
left side (N <sub>4</sub> , C <sub>5</sub> , C <sub>6</sub> , C <sub>7</sub> , N <sub>8</sub> )	6.0 (6.7)	5.9 (6.5)	6.0 (6.7)	5.9 (6.7)

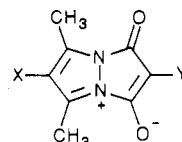
0.6 e<sup>-</sup> (MINDO/3) to 0.8 e<sup>-</sup> (ab initio with STO-3G basis set), with iterative Hückel and ab initio calculations (with 3-21G basis set) both predicting a transfer of 0.7 e<sup>-</sup> upon excitation. Exactly analogous results were obtained for the 2-phenyl derivative 1 and for the 5,7-dimethyl-2-phenyl derivative.

Table X lists visible absorption maxima for the CCMB 8 which show a blue (hypsochromic) shift of 9 nm in changing the solvent from hexane to CH<sub>3</sub>OH. By the arguments of Kosower,<sup>14</sup> a transition that causes a decrease in dipole moment will be disfavored energetically by increased solvent polarity. The result should be an absorption maximum that shifts to shorter wavelengths as the polarity of the solvent increases, and thus the shift observed for 8, although small, is in the proper direction for the predicted charge transfer.

We have also evaluated substituent effects upon the absorption wavelengths. Table XI gives the visible ab-

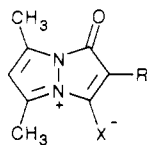
**Table X. Solvent Dependence of the Visible Absorption Maximum in Anhydro-1-hydroxy-5-methyl-3-oxo-2-phenyl-6,7,8,9-tetrahydro-pyrazolo[1,2-a]indazole Hydroxide (8)**

solvent	$\lambda_{\max}$ (nm)	log $\epsilon$
C <sub>6</sub> H <sub>14</sub>	436	—
CH <sub>2</sub> Cl <sub>2</sub>	435	2.94
CH <sub>3</sub> CN	427	3.06
DMSO	429	2.93
CH <sub>3</sub> OH	427	2.79

**Table XI. Visible Absorption Maxima of Various Anhydro-1-hydroxy-3-oxopyrazolo[1,2-a]pyrazolium Hydroxides**

substituents		absorption $\lambda_{\max}$ (nm)
X	Y	
H	<i>p</i> -NO <sub>2</sub> C <sub>6</sub> H <sub>4</sub>	387
H	<i>p</i> -BrC <sub>6</sub> H <sub>4</sub>	394
H	C <sub>2</sub> H <sub>5</sub>	397
H	C <sub>6</sub> H <sub>5</sub>	421
Cl	C <sub>6</sub> H <sub>5</sub>	427
H	<i>p</i> -CH <sub>3</sub> OC <sub>6</sub> H <sub>4</sub>	437
H	<i>p</i> -NH <sub>2</sub> C <sub>6</sub> H <sub>4</sub>	446

sorptions of a series of betaines differing only in the attached substituents. The addition of the electron-withdrawing Br and NO<sub>2</sub> substituents to the para position of the 2-phenyl group causes a hypsochromic shift in the visible absorption maximum as compared to that of the 2-(unsubstituted phenyl) compound 9. In direct contrast to this result is the bathochromic shift obtained upon

**Table XII. Visible Absorption Maxima of Various Anhydro-5,7-dimethyl-1-hydroxy-3-heteropyrazolo[1,2-a]-pyrazolium Hydroxides**

substituents		absorption $\lambda_{\max}$ (nm)
R	X	
C <sub>6</sub> H <sub>5</sub>	O	421
C <sub>6</sub> H <sub>5</sub>	NTos	428
C <sub>6</sub> H <sub>5</sub>	C(CN) <sub>2</sub>	497
C <sub>6</sub> H <sub>5</sub>	S	498
CN	O	360
CN	S	428

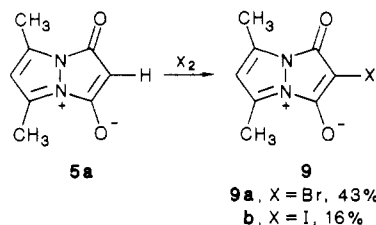
substitution at the same position of the electron-donating OCH<sub>3</sub> and NH<sub>2</sub> substituents. The placement of an electron-withdrawing chlorine atom on C<sub>6</sub> of the CCMB causes a bathochromic shift in the absorption when compared to that of the corresponding unsubstituted compound. These results are in agreement with the predicted transfer of charge from the  $\beta$ -diketone enolate to the pyrazolium ion in such systems. For example, the placement of an electron-withdrawing group on the  $\beta$ -diketone enolate (donor) should impede the electron-transfer process and cause a hypsochromic shift, as observed. The electron-withdrawing chlorine atom on the pyrazolium ion (acceptor), however, should aid in the transfer of charge to that fragment resulting in a bathochromic shift, again as observed.

Hammond<sup>15</sup> has shown that, for intermolecular charge-transfer complexes of hexamethylbenzene with various monosubstituted *p*-benzoquinones, a nearly linear relationship exists between the frequency of the charge-transfer absorption ( $\nu_{CT}$ ) and the Hammett para constant ( $\sigma_p$ ) for the benzoquinone substituent. As the substituents were on the acceptor molecule, an inverse relationship was observed between  $\nu_{CT}$  and  $\sigma_p$ , which measures a group's ability to release, not accept, electrons. In a similar study of intermolecular complexes of tetracyanoethylene (TCNE) and monosubstituted benzenes,<sup>16</sup> the substituents were placed on the donor molecule, and as expected, a direct relationship between  $\nu_{CT}$  and  $\sigma_p$  was observed. A plot of the visible absorption wavelength ( $\lambda_{\max}$ ) of several CCMB related to 8 but differing in the substituent at the para position of the 2-phenyl moiety against the corresponding Hammett  $\sigma_p$  constants showed that a strong inverse correlation exists between these values. Therefore, as wavelength is inversely related to energy,  $\sigma_p$  is directly related to the energy of the absorption process, which is consistent with the placement of the substituents upon the donor species in a charge-transfer system. Our Hammett relationships of these CCMB also provided a  $\pi^*$  value of 0.11 whose magnitude is considered to reflect a relative insensitivity to substituent effects.

The introduction of atoms with different ionization potentials into the  $\beta$ -diketone enolate should have a marked effect upon the ease of electron removal and hence upon the energy of the process. Table XII shows such an effect. The bathochromic shifts in the exocyclic sulfur systems compared to those of their oxygen analogues are due to a lowering of the ionization potential of the donor fragment of the betaines and a lower energy charge-

transfer process. The UV-visible absorption spectra of CCMB and PCCMB remained unchanged in the concentration range 10<sup>-3</sup>-10<sup>-7</sup> M.

**Electrophilic Substitution.** The CCMB 5a undergoes facile electrophilic substitution at C<sub>2</sub> with bromine or iodine to give the halo-CCMB 9 as yellow-orange needles. The molecular ions are the most abundant ions in the electron-impact mass spectra of 9a and 9b, and infrared carbonyl absorption bands at 1785 (weak) and 1715 cm<sup>-1</sup> for 9a, and 1780 (weak) and 1700 cm<sup>-1</sup> for 9b, are characteristic of carbonyl absorption bands in pyrazolium CCMB. This ease of electrophilic substitution is a reflection of the high electron density at C<sub>2</sub>.

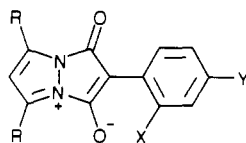


The CCMB 1 also underwent ready electrophilic substitution, e.g., bromination and nitration, in the C<sub>2</sub> phenyl substituent. Such substitution was predicted by the MO calculations above and is consistent with electron delocalization over the phenyl group, which was also indicated by the X-ray data for 1. The betaine 1 and Br<sub>2</sub> in CH<sub>2</sub>Cl<sub>2</sub>/pyridine gave exclusively the *p*-bromo product 10a in 69% yield (Table XIII). The structure of 10a was evident from its analytical and spectral data. The <sup>1</sup>H NMR spectrum (DMSO-*d*<sub>6</sub>) contained a triplet ( $J = 2.63$  Hz) at  $\delta$  7.04 (1 H) and a doublet ( $J = 2.63$  Hz) at  $\delta$  8.84 (2 H), corresponding to the C<sub>6</sub>-H and to the C<sub>5</sub>-H and C<sub>7</sub>-H, respectively. The para substitution pattern is evident from the 2-phenyl hydrogen atoms which are observed as two double doublets ( $J = 6.87$  Hz,  $J = 1.83$  Hz) at  $\delta$  7.51 and 7.95. The addition of pyridine was necessary to remove the HBr formed during the course of the reaction, and in the absence of pyridine, no identifiable product was isolated from the reaction mixture. In contrast to this result, the 5,7-dimethyl system 10 reacted cleanly with Br<sub>2</sub> in CHCl<sub>3</sub> in the absence of pyridine, affording exclusively the para-brominated product 11b in 91% yield (Table XIII).

The exclusive para bromination was not the rule observed in the reaction of these CCMB with HNO<sub>3</sub> in Ac<sub>2</sub>O.<sup>17</sup> The addition of 2 equiv of HNO<sub>3</sub> in Ac<sub>2</sub>O at reduced temperatures to 1 resulted in the exclusive formation of the *o*-nitro product 11c. The spectral data in Table XIII are consistent with this structure, and the NO<sub>2</sub> absorptions were observed at 1580 and 1365 cm<sup>-1</sup>. The aromatic protons' chemical shifts (Experimental Section) were consistent with an ortho-disubstituted benzene. The reaction of the 5,7-dimethyl system 10 under identical conditions resulted in the isolation of two products, the major product being identical in all respects with the *p*-nitro derivative 11e (Table XIII). The second product was determined by its analytical and spectral data to be anhydro-5,7-dimethyl-2-(2,4-dinitrophenyl)-1-hydroxy-3-oxopyrazolo[1,2-a]pyrazolium hydroxide (11d) (Experimental Section). Reduction of the amount of HNO<sub>3</sub> used to 1 equiv resulted once again in the formation of 11e as the major product. The accompanying minor product in this case, however, was not the dinitro derivative 11d but anhydro-5,7-dimethyl-1-hydroxy-2-(2-nitrophenyl)-3-oxo-

(15) Hammond, P. R. *J. Chem. Soc.* 1964, 471.(16) Foster, W. R. *Organic Charge Transfer Complexes*; Academic: New York, 1969.(17) Bordwell, F. G.; Garbisch, E. W. *J. Am. Chem. Soc.* 1960, 82, 3588.

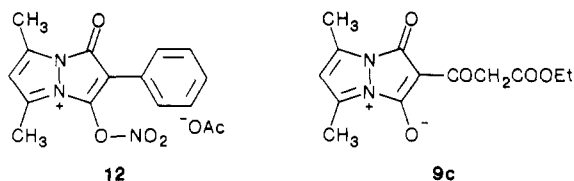
Table XIII. Electrophilic Substitution Reaction of Anhydro-1-hydroxy-3-oxo-2-phenylpyrazolo[1,2-a]pyrazolium Hydroxide



compd no.	R	X	Y	condtns	yield (%)	mp (°C)	M <sup>+</sup> m/z (%)
10a	H	H	Br	Br <sub>2</sub> /CH <sub>2</sub> Cl <sub>2</sub> /pyridine	69	262–264	292 (97), 290 (100)
11b	CH <sub>3</sub>	H	Br	Br <sub>2</sub> /CHCl <sub>3</sub>	91	268–270	320 (98), 318 (100)
11c	H	NO <sub>2</sub>	H	2 equiv of HNO <sub>3</sub> /Ac <sub>2</sub> O	51	330 dec	257 (97)
11d	CH <sub>3</sub>	NO <sub>2</sub>	NO <sub>2</sub>	2 equiv of HNO <sub>3</sub> /Ac <sub>2</sub> O	7	238–242	330 (62)
11e	CH <sub>3</sub>	H	NO <sub>2</sub>	2 equiv of HNO <sub>3</sub> /Ac <sub>2</sub> O	35	>300	285 (100)
11f	CH <sub>3</sub>	NO <sub>2</sub>	H	1 equiv of HNO <sub>3</sub> /Ac <sub>2</sub> O	10	199–200	285 (48)
11e	CH <sub>3</sub>	H	NO <sub>2</sub>	1 equiv of HNO <sub>3</sub> /Ac <sub>2</sub> O	49	>300	285 (100)
11f	CH <sub>3</sub>	NO <sub>2</sub>	H	1 equiv of NaNO <sub>2</sub> /AcOH	51	199–200	285 (48)
11e	CH <sub>3</sub>	H	NO <sub>2</sub>	1 equiv of NaNO <sub>2</sub> /AcOH	42	>300	285 (100)

pyrazolo[1,2-a]pyrazolium hydroxide (11f) (10%).

The reason for this varied regiochemistry in the nitration reaction may be rationalized as follows. The preponderance of ortho substitution in the preparation of 11c is particularly surprising as steric factors associated with such bulky substituents generally direct most electrophiles into the para position in electrophilic aromatic substitution reactions.<sup>18</sup> One possible explanation for this deviation is that the exocyclic oxygen atoms actually aid in the physical direction of the incoming nitro group through an interaction with the nitrating reagent. This interaction may range from simple electronic attraction to actual O-nitration leading to an intermediate of type 12 [related



to the *N*-nitro intermediate predicted in the nitration of anilines<sup>19a</sup> and the *O*-nitro intermediate in the nitration of (methoxyethyl)benzene with N<sub>2</sub>O<sub>5</sub><sup>19b</sup>]. In the case where the 5,7-dimethyl derivative 10 is used, steric interaction with the methyl groups may interfere with the above mechanism, resulting in the formation of a para-substituted compound as the major product. The lack of any ortho substitution in the reaction with Br<sub>2</sub> may be the result of either the increased steric problems due to the extreme bulk of this reagent and/or a simple preference of this reagent for the softer carbon atom over the harder oxygen atom.<sup>18</sup>

The attempted extension of the above nitration procedure to prepare the analogous nitroso derivatives produced unexpected results. In particular, the 5,7-dimethyl derivative 10 with NaNO<sub>2</sub> in AcOH/H<sub>2</sub>O gave the *p*-nitro derivative 11e (42%) and the *o*-nitro derivative 11f (51%) (Table XIII). While the production of nitro compounds under nitrosation conditions is known for active substrates such as amines and phenols, the presence of nitric acid is generally required to oxidize the intermediate nitroso compound to the nitro oxidation state via formation of N<sub>2</sub>O<sub>4</sub>.<sup>21</sup> This result may be indicative of an enhanced

reactivity of the nitroso function on this aromatic ring. This enhanced reactivity may in turn stem from the high electron density that is predicted to reside on the 2-phenyl moiety (as further evidenced by the formation of the dinitro compound 11d under such mild conditions). Attempted nitration of 1 and 10 with HNO<sub>3</sub>/H<sub>2</sub>SO<sub>4</sub> resulted in complete decomposition of the substrate, no identifiable products being isolated.

Further attempts at electrophilic substitution met with less success. In particular, the treatment of 10 with DMF/POCl<sub>3</sub> failed to produce any product; all of the betaine 10 was recovered. In the similar treatment of 10 with acetyl chloride in CS<sub>2</sub>/AlCl<sub>3</sub>, a deep-red precipitate was formed instantly. This precipitate was found to be extremely sensitive to moisture, re-forming the betaine 10 rapidly on exposure to either protic solvents or atmospheric moisture. The further observations that all three reactants (10, acetyl chloride, and AlCl<sub>3</sub>) were essential for the precipitate to form and that the latter two reactants are known to form an extremely electrophilic acylium ion (or equivalent) under these conditions<sup>22</sup> strongly suggest that the product is formed by some kind of association between the betaine 10 and the methylacylium ion. Attempted diazotization of the CCMB was also unsuccessful.

Attempts at similar electrophilic substitution of the CCMB 5b were unsuccessful. Our inability to introduce an acyl group at the C<sub>2</sub> position of 5b, e.g., reaction with malonyl dichloride to give 9c after reaction workup with ethanol, indicates that, in the previous isolation of 9c from the reaction of 3,5-dimethylpyrazole and excess malonyl dichloride/Et<sub>3</sub>N, the acylation must have occurred prior to betaine formation.

**Protonation and Alkylation.** The literature contains many examples of alkylation and protonation of mesomeric betaines (MB) as well as many reports of MB being unreactive toward acids and electrophiles. The CMB 13–15 have all reacted with protic acids and alkylating agents to afford the corresponding cationic heterocycles.<sup>23</sup> In contrast, the CMB 16 and the CCMB 17 have been reported to be unreactive toward protonation and alkylation.<sup>24</sup> The MB that undergo protonation and alkylation do not appear to possess excessive anionic charge localization compared

(21) March, J. *Advanced Organic Chemistry*, 2nd ed.; McGraw-Hill: New York, 1977; p 474.

(22) Reference 21, pp 492–493.

(23) Potts, K. T.; Husain, S. *J. Org. Chem.* 1970, 35, 4351. Ames, D. E.; Kucharska, H. Z. *J. Chem. Soc.* 1963, 4924. Ramsden, C. A.; Ollis, W. D. *J. Chem. Soc., Chem. Commun.* 1976, 306.

(24) Friedrichsen, W.; Kappe, T. *Heterocycles* 1982, 19, 1083. Ollis, W. D.; Ramsden, C. A. *Adv. Heterocycl. Chem.* 1976, 19, 3. Ollis, W. D.; Stanforth, S. P.; Ramsden, C. A. *Tetrahedron* 1985, 41, 2239.

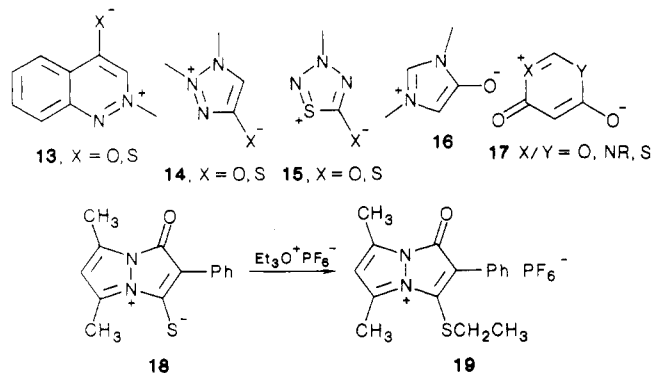
(18) Fleming, I. *Frontier Orbitals and Organic Chemical Reactions*; Wiley: New York, 1976; pp 32, 64.

(19) (a) Ridd, J. H.; Scrivens, E. F. V. *J. Chem. Soc., Chem. Commun.* 1972, 641. (b) Norman, R. O. C.; Radda, G. K. *Proc. Chem. Soc., London* 1960, 423. Norman, R. O. C.; Radda, G. K. *J. Chem. Soc.* 1961, 3030.

(20) Barton, D. H. R.; Ollis, W. D. *Comprehensive Organic Chemistry*; Pergamon: Oxford, 1979; Vol. 4, p 113.



to the MB that do not react, and contrasting the resulting cationic heterocycles provides only a partial rationale.



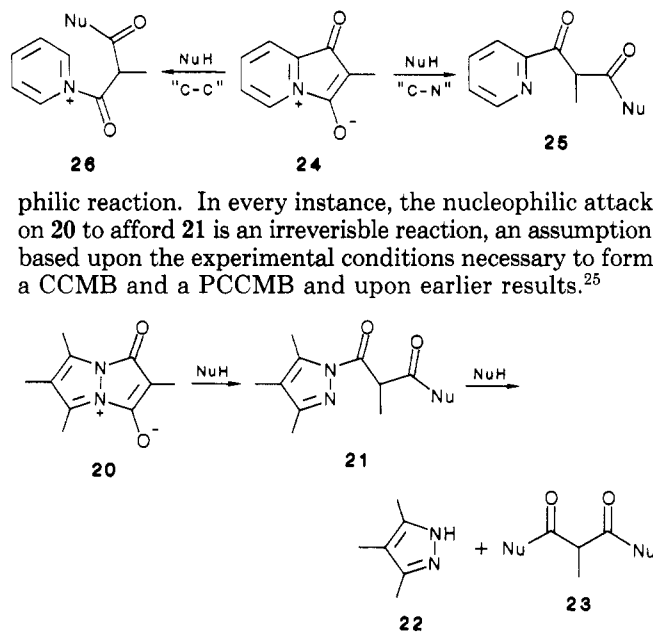
The pyrazolium CCMB **10** and **1** were found to be unreactive to strong, organic and inorganic acids in both aqueous and nonprotic media, including trifluoromethanesulfonic acid, fluorosulfuric acid, tetrafluoroboric acid, picric acid, and perchloric acid. Attempts to isolate the product of protonation of pyrazolium CCMB, as well as  $^1\text{H}$  NMR experiments to detect protonation, were unsuccessful. Similarly, attempts to alkylate **10** with a variety of alkylating agents including methyl iodide, dimethylsulfate, triethylxonium hexafluorophosphate, and ethyl trifluoromethanesulfonate led to no reaction in all instances, **10** being recovered. The only pyrazolium CCMB that underwent alkylation was **18**. While being unreactive toward methyl iodide and dimethyl sulfate, **18** and triethylxonium hexafluorophosphate in  $\text{CH}_2\text{Cl}_2$  at room temperature gave the cationic heterocyclic system **19** (89%). All attempts to protonate or alkylate the other CCMB and PCCMB described in this and the previous paper led to no reaction, with recovery of the unreacted CCMB. The heterocyclic cation system **19** was sensitive to both heat and moisture in solution and was difficult to purify without some decomposition. The structure of **19** was evident from its analytical and spectral data (Experimental Section).

**Reaction with Nucleophiles.** The reaction of CCMB and PCCMB with nucleophiles resulted in cleavage and/or decomposition. In this study we have identified the factors that control their reactivity. Two modes of cleavage of pyrazolium CCMB may operate: cleavage of the pyrazolium ion and cleavage of the "union bonds". The latter pathway was found to predominate except when the pyrazolium ring was unsubstituted.<sup>25</sup>

We have examined the reaction of CCMB and PCCMB with several nucleophiles, these betaines all having visible absorption maxima in the 350–530-nm region. The products of nucleophilic cleavage of "union bonds" in CCMB and PCCMB are malonic acid derivatives (esters, amides, etc.) or  $\beta$ -keto acid derivatives, all of which are colorless crystalline materials, and UV-visible absorption spectroscopy provides a convenient way to monitor the concentration of the CCMB or PCCMB without interference from the reaction products.

In the reaction of pyrazolium CCMB **20** with nucleophiles, such as water, alcohols, amines, etc., the initial CCMB–nucleophile adduct would be the malonic acid derivative **21**, which, under these experimental conditions, was not isolable. Subsequent nucleophilic attack on **21** gave **23** and the corresponding pyrazole **22**. By monitoring of the CCMB concentration, the nucleophilic attack to cleave the CCMB was separated from the second nucleophilic

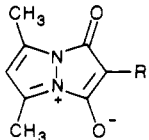
Scheme I. Nucleophilic Cleavage of Pyridinium PCCMB



philic reaction. In every instance, the nucleophilic attack on **20** to afford **21** is an irreversible reaction, an assumption based upon the experimental conditions necessary to form a CCMB and a PCCMB and upon earlier results.<sup>25</sup>

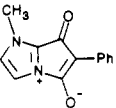
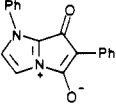
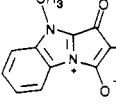
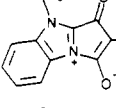
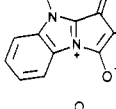
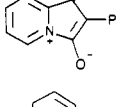
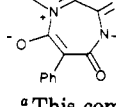
The nucleophilic attack on PCCMB may involve two sites of attack resulting in either carbon–carbon or carbon–nitrogen "union bond" cleavage (Scheme I). In the nucleophilic cleavage of PCCMB, both carbon–carbon and carbon–nitrogen "union bonds" are capable of cleavage leading to decomposition of the PCCMB. Nucleophilic attack at  $\text{C}_3$  will cleave the carbon–nitrogen "union bond" in **24**, affording **25**, an aromatic  $\beta$ -keto acid derivative which would be unreactive toward further nucleophilic attack under these reaction conditions. Alternatively, nucleophilic attack at  $\text{C}_1$  will cleave the carbon–carbon "union bond" and afford the *N*-acylpyridinium derivative **26**, which is expected to react rapidly with nucleophiles to afford **23** and pyridine. By monitoring of the visible absorption maximum of PCCMB during the course of the reaction, the initial nucleophilic cleavage was studied without interference from the subsequent reactions. In the cleavage of PCCMB with nucleophiles, isolation of the final reaction products also revealed details governing their reactivity with nucleophiles.

In the nucleophilic cleavage of CCMB, both "union bonds" are carbon–nitrogen bonds and the observed products were the heterocyclic system and the corresponding malonic acid diamide **23**. In the nucleophilic cleavage of PCCMB, both carbon–carbon and carbon–nitrogen "union bonds" are capable of cleavage leading to decomposition of PCCMB. For triazolium, thiazolium, imidazolium, and pyridinium PCCMB, carbon–carbon "union bond" cleavage dominated the nucleophilic reactivity of PCCMB. The observed products of nucleophilic cleavage of PCCMB were the heterocycle and the corresponding malonic acid diamide **23**, formed by subsequent nucleophilic cleavage of the *N*-acyl heterocyclic cation **26**. If carbon–nitrogen "union bond" cleavage had dominated the nucleophilic reactivity of PCCMB, and theoretical calculations predicted reaction at the amide-like carbonyl carbon atom due to the greater positive charge at that atom, the expected product would be the aromatic ketone **25**, which was not detected in any instance. When only 1 equiv of nucleophile was employed, half of the PCCMB remained unreacted and half was converted into the heterocycle and **23**. CCMB containing a pyrazolium nucleus but with no 2-substituent, or with ester groups in the pyrazole ring, were too reactive with water to measure the

**Table XIV. Kinetic Measurements: Nucleophilic Cleavage of Pyrazolium CCMB**


R	second-order rate constant (M <sup>-1</sup> s <sup>-1</sup> ) for nucleophile	
	C <sub>6</sub> H <sub>5</sub> NH <sub>2</sub>	morpholine
C <sub>6</sub> H <sub>5</sub>		1.2 × 10 <sup>-4</sup>
CH <sub>2</sub> CH <sub>3</sub>	8.8 × 10 <sup>-6</sup>	3.5 × 10 <sup>-3</sup>
Br	5.6 × 10 <sup>-6</sup>	1.9 × 10 <sup>-3</sup>
CN		5.0 × 10 <sup>-3</sup>
CH <sub>2</sub> CH=CH <sub>2</sub>		5.7 × 10 <sup>-3</sup>
C(CH <sub>3</sub> )=CH <sub>2</sub>		3.2 × 10 <sup>-4</sup>

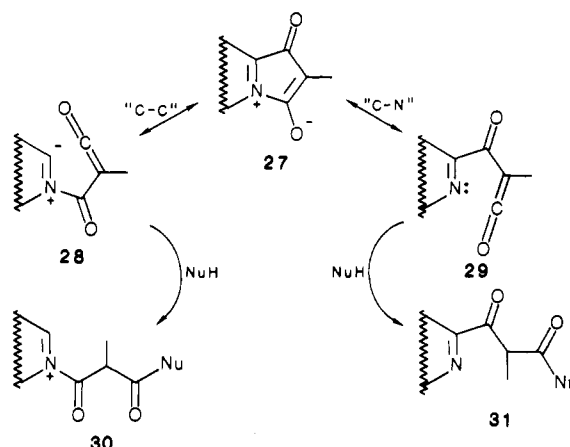
**Table XV. Kinetic Measurements: Nucleophilic Cleavage of PCCMB**

PCCMB	second-order rate constant (M <sup>-1</sup> s <sup>-1</sup> ) for nucleophile		
	water	C <sub>6</sub> H <sub>5</sub> NH <sub>2</sub>	morpholine
		9.9 × 10 <sup>-5</sup>	2.2 × 10 <sup>-2</sup>
	1.1 × 10 <sup>-6</sup>	1.3 × 10 <sup>-3</sup>	
		6.8 × 10 <sup>-5</sup>	
	2.9 × 10 <sup>-5</sup>	4.6 × 10 <sup>-3</sup>	
		5.2 × 10 <sup>-3</sup>	
			2.0 × 10 <sup>-6</sup>
		4.8 × 10 <sup>-3</sup>	

<sup>a</sup>This compound is a CCMB.

kinetics of the reaction. This was also found for CCMB containing the 1,2,3- and 1,2,4-triazole nuclei as well as for PCCMB derived from 1-methylimidazole and having no 2-substituent or a 2-ethyl substituent, 1,2,4-triazoles, and benzothiazoles. Table XIV shows kinetic data for the nucleophilic cleavage of a series of pyrazolium CCMB, and similar data are shown in Table XV for a series of PCCMB.

Valence tautomerization plays an important role in the chemistry of many MB, and while no chemical or spectroscopic evidence for valence tautomerization in CCMB or PCCMB to heterocyclic ketenes has been observed, the ketene resonance contributors **28** and **29** to the betaine **27** explain the elongated "union bonds" in CCMB and PCCMB as well as their susceptibility to nucleophilic

**Scheme II. Models for Nucleophilic Cleavage of "Union Bonds" in CCMB and PCCMB**

cleavage. By assuming that a greater ketene resonance contribution leads to greater reactivity with nucleophiles, we developed qualitative models to compare the extent of "no bond resonance" in CCMB and PCCMB and their susceptibility to nucleophilic cleavage.

The more basic nitrogen atom in **29**, the less **29** would be expected to contribute to the properties of the CCMB or PCCMB **27**, and consequently **27** is less reactive toward carbon-nitrogen "union bond" cleavage. The basicity of the nitrogen atom in **29** can be approximated by the basicity of the corresponding heterocycle. The basicity of the heterocycle is also an indication of the heterocyclic cation stability, and a more stable heterocyclic cation moiety results in a more stable CCMB or PCCMB. In CCMB, carbon-nitrogen "union bond" cleavage dominates their nucleophilic reactions. Pyrazolium CCMB are much less reactive than triazolium CCMB, and the reactivity of CCMB parallels the basicity of the heterocyclic system, pyrazoles ( $pK_a \sim 2.3$ ) being more basic than 1,2,3-triazoles<sup>26</sup> ( $pK_a \sim 1.1$ ). The basicity of 1,2,4-triazoles ( $pK_a \sim 3.2$ ) contains an additional complexity. 1,2,4-Triazoles protonate at N<sub>1</sub> and N<sub>4</sub>, i.e., the imidazolium-like ion, and no physical measurements can be made of protonation at N<sub>1</sub> and N<sub>2</sub>, i.e., the pyrazolium-like ion, present in CCMB. Theoretical values for protonation at N<sub>1</sub> and N<sub>2</sub> in 1,2,4-triazoles predict values for the  $pK_a \sim 1.3$  approximately equal to that of the 1,2,3-triazolium systems.<sup>27</sup>

The pyrazolium CCMB containing diester substituents in the pyrazolium moiety were also susceptible to nucleophilic cleavage. Gonzalez's work<sup>28</sup> predicts  $pK_a$  values for the corresponding diester derivatives of pyrazole in the range -6.3 to -4.8. Thus, electron-withdrawing groups in the cationic fragment of CCMB facilitate carbon-nitrogen "union bond" cleavage by nucleophiles.

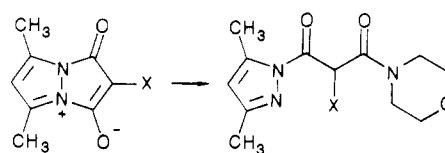
The susceptibility of carbon-carbon "union bonds" in CCMB and PCCMB to nucleophilic cleavage (the conversion of **27** into **30**) is modeled by the valence tautomerization between **27** and **28** (Scheme II). The relative contribution of the ylidic species **28** to the properties of the MB **27** was approximated by the rate of hydrogen/deuterium exchange at the  $\alpha$  carbon atom in the corresponding cationic heterocycle, in which the ylidic species **32** is the reaction intermediate.<sup>29</sup> A more rapid rate of exchange corresponds to a lower energy ylidic intermediate

(26) Schofield, K.; Grimmett, M. R.; Keene, B. R. T. In *The Azoles*; Cambridge University: London, 1976.

(27) Vaughan, J. D.; O'Donnell, M. *Tetrahedron Lett.* 1968, 3727.

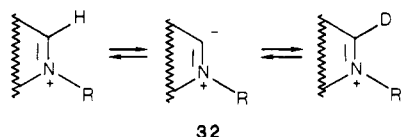
(28) Gonzalez, E. *Bull. Chim. Soc. Fr.* 1968, 5009.

(29) Schroeder, M. A.; Makino, R. C. *Tetrahedron* 1973, 29, 3469.

**Table XVI. Influence of Substituents on Nucleophilic Cleavage of Pyrazolium CCMB**


X	ln $k_{2nd}$	rel rate	Hammett $\sigma_{para}$	Taft $E_s$
CH <sub>2</sub> CH=CH <sub>2</sub>	-5.16	47	-0.13	-1.5
CN	-5.30	41	0.66	-0.51
CH <sub>2</sub> CH <sub>3</sub>	-5.65	29	-0.15	-1.31
Br	-6.28	15	0.23	-1.16
C(CH <sub>3</sub> )=CH <sub>2</sub>	-8.05	2.6	-0.03	-3.32
C <sub>6</sub> H <sub>5</sub>	-9.02	1	-0.01	-3.79
H	>>0	-	0	0

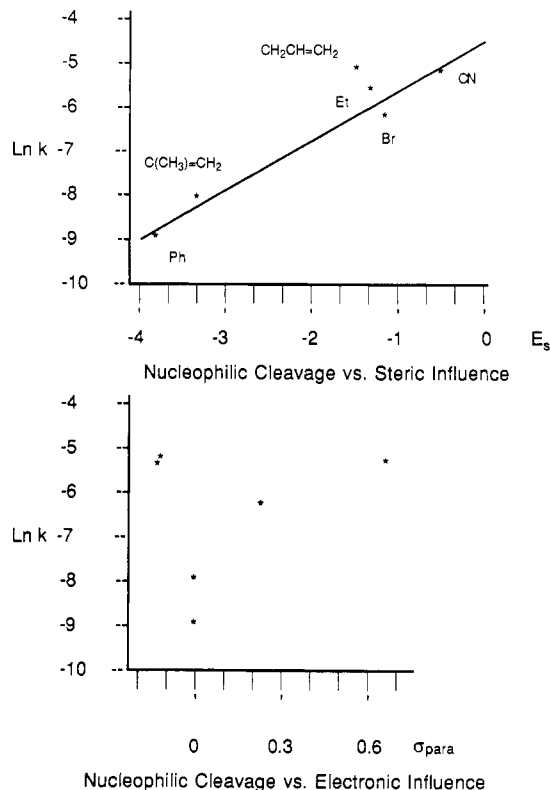
32. Analogously, the tautomer **28** contributes to the properties of the CCMB or PCCMB according to its relative energetics.



All PCCMB underwent carbon-carbon "union bond" nucleophilic cleavage, pyridinium PCCMB being less reactive than imidazolium and benzimidazolium PCCMB, which, in turn, were less reactive than benzothiazolium and 1,2,4-triazolium PCCMB. The reactivity of PCCMB with nucleophiles corresponds to the rate of hydrogen/deuterium exchange in the corresponding cationic heterocycle,<sup>30</sup> pyridinium ions [ $k_{2nd}$  (C-H/D) = 0.2 M<sup>-1</sup> s<sup>-1</sup>] being less reactive than the imidazolium ions [ $k_{2nd}$  (C-H/D) = 300 M<sup>-1</sup> s<sup>-1</sup>] and the benzimidazolium ions [ $k_{2nd}$  (C-H/D) = 4 × 10<sup>4</sup> M<sup>-1</sup> s<sup>-1</sup>], which were less reactive than thiazolium ion [ $k_{2nd}$  (C-H/D) = 1 × 10<sup>6</sup> M<sup>-1</sup> s<sup>-1</sup>], benzothiazolium [ $k_{2nd}$  (C-H/D) = 3 × 10<sup>9</sup> M<sup>-1</sup> s<sup>-1</sup>], and 1,2,4-triazolium ions [ $k_{2nd}$  (C-H/D) = 5 × 10<sup>7</sup> M<sup>-1</sup> s<sup>-1</sup>].

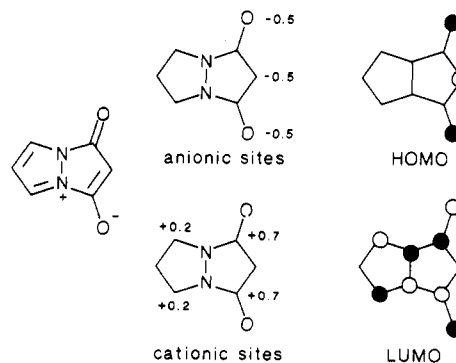
The influence of substituents at C<sub>2</sub> in the anionic fragment of pyrazolium CCMB is summarized in Table XVI. These results demonstrate that the reactivity of pyrazolium CCMB with morpholine is essentially independent of the electronic nature of the substituent at C<sub>2</sub> in the anionic fragment of pyrazolium CCMB. The steric influence of the substituent at C<sub>2</sub> correlates well to the reactivity of pyrazolium CCMB with nucleophiles, a larger substituent at C<sub>2</sub> being less susceptible to nucleophilic cleavage.

The plot of ln  $k$  vs  $E_s$  (Figure 3) for the family of pyrazolium CCMB, except for **5a**, produces a straight line with a slope of 1.2 and a correlation of 94%. The slope indicates a reaction mechanism 20% more sensitive to steric influence than that in Taft's investigation<sup>31</sup> of the saponification of XCH<sub>2</sub>COOR. The rate of nucleophilic cleavage of pyrazolium CCMB unsubstituted at C<sub>2</sub> (**5a**) is significantly more rapid than that predicted by an examination of the steric influence of a hydrogen substituent. The accelerated nucleophilic decomposition of **5** and **5a** suggests that an alternative mechanism governs their reactivity, though the products isolated from the nucleophilic cleavage of **5** and **5a** were the expected products of nucleophilic attack at the carbonyl carbon atoms leading to carbon-nitrogen "union bond" cleavage.

**Figure 3.**

### Conclusions

We have shown that cross-conjugated (CCMB) and pseudo-cross-conjugated (PCCMB) mesomeric betaines contain distinct anionic and cationic segments which comprise a common  $\pi$ -electron system. Many of the properties of CCMB and PCCMB are attributed to the specific cationic and anionic portions of these zwitterions and to the weak nature of the "union bonds" which join the cationic fragment to nodal positions in the HOMO of the anionic fragment. A summary of the properties of anhydro-1-hydroxy-3-oxopyrazolo[1,2-*a*]pyrazolium hydroxide is shown in the figures and is typical of CCMB and PCCMB.



The charge distribution in the anionic segments accounts for the alkylation of CCMB and PCCMB and their ability to undergo electrophilic substitution. The electron-deficient carbonyl carbon atoms, the weak nature of the "union bonds", and the presence of a neutral heterocycle as the leaving group account for the susceptibility of CCMB and PCCMB to nucleophilic cleavage. The spectroscopic characteristics of CCMB and PCCMB include the upfield NMR shift of C<sub>2</sub> and substituents attached at C<sub>2</sub>, the deep colors associated with intramolecular charge transfer bands, mass spectra containing a prominent molecular ion

(30) Zoltewicz, J. A.; Helmick, L. S. *J. Am. Chem. Soc.* **1970**, *92*, 7542. Olofson, R. A. *J. Am. Chem. Soc.* **1964**, *86*, 1865.

(31) Charton, M. *J. Am. Chem. Soc.* **1975**, *97*, 1552. Charton, M. *J. Org. Chem.* **1976**, *41*, 2217.

and fragmentation associated with cleavage of the "union bonds", and large dipole moments.

### Experimental Section<sup>32</sup>

**Anhydro-2-bromo-5,7-dimethyl-1-hydroxy-3-oxopyrazolo[1,2-a]pyrazolium Hydroxide (9a).** At 0 °C under N<sub>2</sub>, a solution of anhydro-5,7-dimethyl-1-hydroxy-3-oxopyrazolo[1,2-a]pyrazolium hydroxide (0.33 g, 2.0 mmol) in THF (25 mL) was treated with Br<sub>2</sub> (0.35 g, 2.0 mmol). After being stirred for 15 min, the mixture was filtered and the filtrate concentrated in vacuo to a waxy, yellow solid. The addition of ether produced yellow-orange needles, which were filtered and allowed to air-dry: yield 0.21 g (43%); mp 165–180 °C dec; IR (KBr) 1785 (CO), 1715 (CO), 1690 (CO) cm<sup>-1</sup>; UV-vis λ<sub>max</sub> 400 nm (CH<sub>2</sub>Cl<sub>2</sub>); <sup>1</sup>H NMR (CDCl<sub>3</sub>) δ 6.21 (s, 1, C<sub>6</sub>-H), 2.65 (s, 6, 2 × CH<sub>3</sub>); <sup>13</sup>C NMR (CDCl<sub>3</sub>) 156.6, 144.7, 111.4, 59.7, 11.3 ppm; mass spectrum, *m/z* (relative intensity) M<sup>+</sup> 244 (<sup>81</sup>Br, 100), and 242 (<sup>79</sup>Br, 99), 216 (19), 214 (19), 149 (47), 147 (46), 121 (11), 119 (11), 107 (46), 95 (63), 93 (16), 91 (16), 67 (43).

Anal. Calcd for C<sub>8</sub>H<sub>7</sub>BrN<sub>2</sub>O<sub>2</sub>: C, 39.53; H, 2.90; N, 11.53. Found: C, 39.46; H, 2.92; N, 11.47.

**Anhydro-5,7-dimethyl-1-hydroxy-2-iodo-3-oxopyrazolo[1,2-a]pyrazolium Hydroxide (9b).** A solution of anhydro-5,7-dimethyl-1-hydroxy-3-oxopyrazolo[1,2-a]pyrazolium hydroxide (0.24 g, 1.5 mmol) in CH<sub>2</sub>Cl<sub>2</sub> (20 mL) was treated with a solution of I<sub>2</sub> (0.70 g, 4.0 mmol) in CH<sub>2</sub>Cl<sub>2</sub> (20 mL) at room temperature. After being stirred for 60 min, the reaction mixture was purified by chromatography on silica using hexane/CH<sub>2</sub>Cl<sub>2</sub> and eventually ether as the eluent system. Evaporation of the solvent under reduced pressure from the second fraction (yellow band) afforded the product as yellow prisms: 0.07 g (16%); mp 150–153 °C dec; IR (KBr) 1780 (sh, CO), 1720 (sh, CO), 1700 (CO) cm<sup>-1</sup>; <sup>1</sup>H NMR (CDCl<sub>3</sub>) δ 6.15 (s, 1, C<sub>6</sub>-H), 2.65 (s, 6, 2 × CH<sub>3</sub>); mass spectrum, *m/z* (relative intensity) M<sup>+</sup> 290 (100), 291 (9), 195 (41), 167 (8), 139 (14), 127 (20), 107 (10), 95 (33), 67 (35).

**Anhydro-2-(4-bromophenyl)-1-hydroxy-3-oxopyrazolo[1,2-a]pyrazolium Hydroxide (10a).** A stirred solution of pyridine (0.8 g, 0.9 mmol) and anhydro-1-hydroxy-3-oxo-2-phenylpyrazolo[1,2-a]pyrazolium hydroxide (1.06 g, 5 mmol) in CH<sub>2</sub>Cl<sub>2</sub> (30 mL) was treated with Br<sub>2</sub> (0.30 mL, 6 mmol). After 18 h, the precipitate was collected, washed with H<sub>2</sub>O and CH<sub>3</sub>OH, and air-dried. Recrystallization from CH<sub>3</sub>CN afforded the product as maroon prisms: 1.0 g (69%); mp 262–264 °C dec; IR (KBr) 1770 (w), 1735 (w), 1700 (br), 1655 (CO) cm<sup>-1</sup>; UV-vis λ<sub>max</sub> (C<sub>2</sub>H<sub>5</sub>CN) nm (log ε) 210 (4.52), 274 (4.49), 433 (3.06); <sup>1</sup>H NMR (200 MHz) (DMSO-*d*<sub>6</sub>) δ 7.04 (t, 1, J<sub>5,6</sub> = J<sub>6,7</sub> = 2.63 Hz, C<sub>6</sub>-H), 7.51 (dd, 2, J<sub>2,3</sub> = J<sub>5,6</sub> = 6.87 Hz, J<sub>2,5</sub> = J<sub>3,6</sub> = 1.83 Hz, phenyl C<sub>2</sub>-H and C<sub>6</sub>-H), 7.95 (dd, 2, J<sub>2,3</sub> = J<sub>5,6</sub> = 6.87 Hz, J<sub>2,5</sub> = J<sub>3,6</sub> = 1.83 Hz, phenyl C<sub>2</sub>-H and C<sub>5</sub>-H), 8.84 (d, 2, J<sub>5,6</sub> = J<sub>6,7</sub> = 2.63 Hz, C<sub>5</sub>-H and C<sub>7</sub>-H); <sup>13</sup>C NMR (DMSO-*d*<sub>6</sub>) 79.5, 112.1, 115.9, 124.9, 129.6, 130.8, 131.7, 157.5 ppm; mass spectrum, *m/z* (relative intensity) M<sup>+</sup> 290 (100), 291 (17) (M + 1), 292 (97) (M + 2), 293 (15) (M + 3), 225 (16), 224 (23), 223 (17), 222 (22), 197 (30), 195 (30), 183 (11), 181 (11), 169 (37), 167 (37), 102 (10), 88 (39), 62 (10).

Anal. Calcd for C<sub>12</sub>H<sub>7</sub>BrN<sub>2</sub>O<sub>2</sub>: C, 49.51; H, 2.42; N, 9.62. Found: C, 49.38; H, 2.44; N, 9.61.

**Anhydro-2-(4-bromophenyl)-5,7-dimethyl-1-hydroxy-3-oxopyrazolo[1,2-a]pyrazolium Hydroxide (11b).** A stirred suspension of anhydro-5,7-dimethyl-1-hydroxy-3-oxo-2-phenylpyrazolo[1,2-a]pyrazolium hydroxide (2.40 g, 10 mmol) in CHCl<sub>3</sub> (40 mL) was treated with Br<sub>2</sub> (0.5 mL, 10 mmol). A thick precipitate formed, and HBr was evolved. After 18 h, the solvent was removed under reduced pressure. Recrystallization of the residual red solid from CH<sub>3</sub>CN afforded the product as orange-red spears: 2.9 g (91%); mp 268–270 °C; IR (KBr) 1670 (CO) cm<sup>-1</sup>; UV-vis λ<sub>max</sub> (CH<sub>3</sub>CN) nm (log ε) 213 (4.47), 278 (4.50), 422 (2.94); <sup>1</sup>H NMR (200 MHz) (CDCl<sub>3</sub>) δ 2.69 (s, 6, 2 × CH<sub>3</sub>), 6.19 (s, 1, C<sub>6</sub>-H), 7.45 (d, 2, J = 8.78 Hz, phenyl C<sub>2</sub>-H and C<sub>6</sub>-H), 7.98 (d, 2, J = 8.78 Hz, phenyl C<sub>3</sub>-H and C<sub>5</sub>-H); <sup>13</sup>C NMR (CDCl<sub>3</sub>) 11.2, 81.6, 111.8, 117.4, 118.0, 125.7, 131.1, 143.3, 159.0 ppm; mass spectrum, *m/z* (relative intensity) M<sup>+</sup> 318 (100), 319 (18) (M +

1), 320 (98) (M + 2), 321 (17) (M + 3), 225 (15), 223 (17), 197 (21), 195 (21), 169 (25), 176 (23), 95 (23), 89 (11).

Anal. Calcd for C<sub>14</sub>H<sub>11</sub>BrN<sub>2</sub>O<sub>2</sub>: C, 52.69; H, 3.47; N, 8.78. Found: C, 52.84; H, 3.49; N, 8.74.

**Anhydro-1-hydroxy-2-(2-nitrophenyl)-3-oxopyrazolo[1,2-a]pyrazolium Hydroxide (11c).** Concentrated nitric acid (70%) (0.9 g, 10 mmol) was added with stirring to acetic anhydride (15 mL). The mixture was cooled in a dry ice/acetone bath until the mixture became slushy, the cooling bath was then removed, and anhydro-1-hydroxy-3-oxo-2-phenylpyrazolo[1,2-a]pyrazolium hydroxide (1.06 g, 5 mmol) was added. The mixture was stirred until all visible traces of the starting material were replaced by a fine orange precipitate, which was collected, washed with AcOH, and air-dried. The product was finally obtained as orange-red needles by recrystallization from DMF: 0.65 g (51%); mp 330 °C dec; IR (KBr) 1765 (w), 1740 (w), 1705 (br) (CO), 1580 (s), 1365 (s) (NO<sub>2</sub>) cm<sup>-1</sup>; UV-vis λ<sub>max</sub> (DMF) nm (log ε) 383 (4.12); <sup>1</sup>H NMR (200 MHz) (CDCl<sub>3</sub>) δ 6.81 (t, 1, J<sub>5,6</sub> = J<sub>6,7</sub> = 2.54 Hz, C<sub>6</sub>-H), 7.36 (ddd, 1, J<sub>3,4</sub> = 8.32 Hz, J<sub>4,5</sub> = 7.52 Hz, J<sub>4,6</sub> = 1.21 Hz, phenyl C<sub>4</sub>-H), 7.60 (ddd, 1, J<sub>5,6</sub> = 7.71 Hz, J<sub>4,6</sub> = 1.21 Hz, phenyl C<sub>6</sub>-H), 7.91 (dd, 1, J<sub>3,4</sub> = 8.32 Hz, J<sub>3,5</sub> = 1.25 Hz, phenyl C<sub>3</sub>-H), 8.13 (d, 2, J<sub>5,6</sub> = J<sub>6,7</sub> = 2.54 Hz, C<sub>5</sub>-H and C<sub>7</sub>-H); mass spectrum, *m/z* (relative intensity) M<sup>+</sup> 257 (97), 258 (14) (M + 1), 213 (34), 212 (10), 211 (12), 190 (19), 186 (13), 185 (78), 171 (59), 159 (12), 157 (11), 156 (23), 147 (18), 146 (100), 143 (10), 134 (23), 131 (15), 119 (18), 104 (18), 103 (18), 102 (10), 95 (11), 92 (11), 90 (73), 88 (18), 76 (11), 68 (31), 64 (17), 63 (24), 44 (77), 41 (11), 40 (10), 39 (20).

Anal. Calcd for C<sub>12</sub>H<sub>9</sub>N<sub>3</sub>O<sub>4</sub>: C, 56.05; H, 2.72; N, 16.34. Found: C, 56.11; H, 2.78; N, 16.33.

**Reaction of Anhydro-5,7-dimethyl-1-hydroxy-3-oxo-2-phenylpyrazolo[1,2-a]pyrazolium Hydroxide with 2 equiv of Acetyl Nitrate.** Concentrated nitric acid (70%) (1.80 g, 20 mmol) was added with stirring to ice-cold Ac<sub>2</sub>O (25 mL). The cooling bath was removed, and anhydro-5,7-dimethyl-1-hydroxy-3-oxo-2-phenylpyrazolo[1,2-a]pyrazolium hydroxide (2.40 g, 10 mmol) was added. The mixture was stirred until all visible traces of the starting material were replaced with a fine orange precipitate, which was then collected (the filtrate was saved for isolation of a second product, described below). The solid was washed with AcOH, air-dried, and recrystallized from DMSO to give anhydro-5,7-dimethyl-1-hydroxy-2-(4-nitrophenyl)-3-oxopyrazolo[1,2-a]pyrazolium hydroxide as orange needles: 1.0 g (35%); mp >300 °C. Spectral data were identical in all respects to those above.

To the filtrate from the reaction mixture was added CH<sub>3</sub>OH (20 mL) to destroy excess Ac<sub>2</sub>O. The solvent was removed under reduced pressure and the resulting oil triturated with Et<sub>2</sub>O. The solid that formed was collected, washed with Et<sub>2</sub>O, and air-dried, resulting in anhydro-5,7-dimethyl-2-(2,4-dinitrophenyl)-1-hydroxy-3-oxopyrazolo[1,2-a]pyrazolium hydroxide as an orange powder: 200 mg (7%); mp 238–242 °C dec; IR (KBr) 1680 (CO) cm<sup>-1</sup>; <sup>1</sup>H NMR (200 MHz) (CDCl<sub>3</sub>) δ 2.73 (s, 6, 2 × CH<sub>3</sub>), 6.32 (s, 1, C<sub>6</sub>-H), 8.13 (d, 1, J<sub>5,6</sub> = 8.88 Hz, phenyl C<sub>6</sub>-H), 8.37 (dd, 1, J<sub>5,6</sub> = 8.88 Hz, J<sub>3,5</sub> = 2.42 Hz, phenyl C<sub>5</sub>-H), 8.71 (d, 1, J<sub>3,5</sub> = 2.42 Hz, phenyl C<sub>3</sub>-H); <sup>13</sup>C NMR (CDCl<sub>3</sub>) 11.4, 80.9, 112.6, 120.9, 126.2, 130.3, 132.4, 144.1, 144.7, 146.4, 157.4 ppm; mass spectrum, *m/z* (relative intensity) M<sup>+</sup> 330 (62), 286 (16), 274 (30), 258 (30), 212 (15), 198 (20), 184 (12), 179 (14), 149 (18), 123 (100), 103 (14), 101 (10), 95 (14), 89 (16), 87 (20), 86 (10), 82 (21), 75 (15).

Anal. Calcd for C<sub>14</sub>H<sub>10</sub>N<sub>4</sub>O<sub>6</sub>: C, 50.92; H, 3.05; N, 16.96. Found: C, 50.75; H, 3.09; N, 16.94.

**Reaction of Anhydro-5,7-dimethyl-1-hydroxy-3-oxo-2-phenylpyrazolo[1,2-a]pyrazolium Hydroxide with 1 equiv of Acetyl Nitrate.** Concentrated nitric acid (70%) (450 mg, 5 mmol) was added with stirring to ice-cold Ac<sub>2</sub>O (20 mL). The cooling bath was removed, and anhydro-5,7-dimethyl-1-hydroxy-3-oxo-2-phenylpyrazolo[1,2-a]pyrazolium hydroxide (1.20 g, 5 mmol) was added. The mixture was stirred until all visible traces of the starting material were replaced with a fine orange precipitate, which was then collected (the filtrate was saved for isolation of a second product, described below). The solid was washed with AcOH, air-dried, and recrystallized from DMSO to give anhydro-5,7-dimethyl-1-hydroxy-2-(4-nitrophenyl)-3-oxopyrazolo[1,2-a]pyrazolium hydroxide as orange needles: 700 mg (49%); mp >300 °C. Spectral data were identical in all respects with those above.

(32) Knorr, L.; Rosengarten, G. D. *Justus Liebigs Ann. Chem.* 1894, 279, 237.

To the filtrate from the reaction mixture was added  $\text{CH}_3\text{OH}$  (20 mL) to destroy excess  $\text{Ac}_2\text{O}$ . The solvent was removed under reduced pressure and the resulting oil triturated with  $\text{Et}_2\text{O}$ . The solid that formed was collected, washed with  $\text{Et}_2\text{O}$ , and air-dried. Recrystallization from  $\text{EtOH}$  afforded anhydro-5,7-dimethyl-1-hydroxy-2-(2-nitrophenyl)-3-oxopyrazolo[1,2-*a*]pyrazolium hydroxide as orange needles: 140 mg (10%); mp 199–200 °C; IR (KBr) 1670 (CO)  $\text{cm}^{-1}$ ;  $^1\text{H}$  NMR (200 MHz) ( $\text{CDCl}_3$ )  $\delta$  2.68 (s, 6, 2  $\times$   $\text{CH}_3$ ), 6.23 (s, 1,  $\text{C}_6\text{-H}$ ), 7.30 (td, 1,  $J_{3,4'} = 8.03$  Hz,  $J_{4,5'} = 7.63$  Hz,  $J_{4,6'} = 1.45$  Hz, phenyl  $\text{C}_4\text{-H}$ ); 7.56 (td, 1,  $J_{4,5'} = 7.63$  Hz,  $J_{5,6'} = 7.83$  Hz,  $J_{3,5'} = 1.41$  Hz, phenyl  $\text{C}_5\text{-H}$ ), 7.82 (dd, 1,  $J_{5,6'} = 7.83$  Hz,  $J_{4,6'} = 1.45$  Hz, phenyl  $\text{C}_6\text{-H}$ ), 7.86 (dd, 1,  $J_{3,4'} = 8.03$  Hz,  $J_{3,5'} = 1.41$  Hz, phenyl  $\text{C}_2\text{-H}$ );  $^{13}\text{C}$  NMR ( $\text{CDCl}_3$ ) 11.2, 80.7, 112.0, 124.8, 125.2, 125.9, 130.6, 132.2, 144.0, 147.8, 158.2 ppm; mass spectrum,  $m/z$  (relative intensity)  $\text{M}^{+\cdot}$  285 (48), 241 (10), 240 (22), 229 (23), 213 (28), 199 (16), 185 (10), 184 (25), 146 (15), 134 (31), 123 (100), 117 (12), 104 (35), 102 (10), 90 (38), 89 (16), 88 (23), 82 (21), 76 (19), 63 (21), 62 (15), 39 (18).

Anal. Calcd for  $\text{C}_{14}\text{H}_{11}\text{N}_3\text{O}_4$ : C, 58.95; H, 3.89; N, 14.73. Found: C, 59.05; H, 3.91; N, 14.71.

**5,7-Dimethyl-3-(ethylthio)-2-phenyl-1-oxopyrazolo[1,2-*a*]pyrazolium Hexafluorophosphate (19).** A stirred solution of anhydro-5,7-dimethyl-1-hydroxy-2-phenyl-3-thioxopyrazolo[1,2-*a*]pyrazolium hydroxide (0.5 g, 2.0 mmol) in dry  $\text{CH}_2\text{Cl}_2$  (20 mL) was treated with triethylxonium hexafluorophosphate (0.55 g, 2.2 mmol). The color changed instantly from deep purple to deep yellow-brown. After 18 h, the solvent was partially removed under reduced pressure and dry  $\text{Et}_2\text{O}$  (25 mL) was added. The resulting mustard-colored precipitate was collected and the product finally obtained as orange needles by recrystallization from  $\text{CH}_2\text{Cl}_2/\text{CCl}_4$  without heating: 0.75 g (89%); mp 146–151 °C dec; IR (KBr) 1770 (CO)  $\text{cm}^{-1}$ ; UV-vis  $\lambda_{\text{max}}$  ( $\text{CH}_2\text{CN}$ ) nm (log  $\epsilon$ ) 255 (4.07), 302 (3.93), 429 (3.41);  $^1\text{H}$  NMR (200 MHz) ( $\text{CDCl}_3$ )  $\delta$  1.20 (t, 3,  $J = 7.32$  Hz,  $\text{SCH}_2\text{CH}_3$ ), 2.73 (s, 3,  $\text{CH}_3$ ), 2.84 (s, 3,  $\text{CH}_3$ ), 2.85 (q, 2,  $J = 7.37$  Hz,  $\text{SCH}_2\text{CH}_3$ ), 6.56 (s, 1,  $\text{C}_6\text{-H}$ ), 7.60–7.48 (m, 3, aromatic), 7.72–7.63 (m, 2, aromatic); mass spectrum,  $m/z$  (relative intensity)  $\text{M}^{+\cdot}$  284 (23), 255 (13), 220 (13), 161 (11), 133 (14), 107 (100), 96 (21), 95 (20), 89 (13), 88 (15).

Anal. Calcd for  $\text{C}_{16}\text{H}_{17}\text{F}_6\text{N}_2\text{OPS}$ : C, 44.66; H, 3.98; N, 6.51. Found: C, 44.74; H, 4.01; N, 6.48.

**Experimental Procedure for Determination of Dipole Moments.** The method used for the determination of dipole moments was that of Guggenheim and Smith. This procedure is based on the calculation of  $P_{20}$  from the equation

$$P_{20} = \frac{4\pi N}{9kT} \mu^2 = \frac{3M}{d} \left( \frac{\alpha}{(\epsilon_1 + 2)^2} + \frac{\gamma}{(n_1^2 + 2)^2} \right)$$

which is based on the Debye equation, and  $\alpha$  is determined from the slope of the line obtained by plotting the dielectric against the weight fraction. Similarly,  $\gamma$  is determined by plotting the refractive index squared against the weight fraction.

After obtaining  $P_{20}$  for a molecule, the expression

$$\mu = 0.01283(P_{20}T)^{0.5}$$

is used to determine the dipole moment. The value 0.01283 will give dipole moments in debye units.

The accuracy of the dipole moments was determined by using the analysis presented by Sutton. This analysis is based on the following simplified equation of the dipole moment:

$$\mu = M^{0.5}(0.092\alpha - 0.0279\gamma + 0.0017)^{0.5}$$

Taking the appropriate derivatives leads to the following:

$$\frac{\partial \mu}{\partial \alpha} = M^{0.5}(0.092\alpha - 0.0279\gamma + 0.0017)^{-0.5}(0.0046)$$

which was used to determine the accuracy of the tests from the equation

$$\frac{\partial \mu}{\partial \gamma} = M^{0.5}(0.092\alpha - 0.0279\gamma + 0.0017)^{-0.5}(0.014)$$

Dielectric constants were measured in a benzene solution by using a Wissenschaftliche Technische Werksstätten Dipolmeter DM01. Benzene (sulfur free) was purified by distillation from sodium metal. The index of refraction was measured by using a Bausch

& Lomb refractometer at the Na D line. Weight fractions were in the range 0.001–0.015 g/mL.

**Procedure for Measuring the Kinetics of the Reaction of CCMB and PCCMB with Nucleophiles.** A THF solution of the CCMB or PCCMB and a known amount of the nucleophile (water, aniline, or morpholine) was prepared in a volumetric flask. The initial absorptivity measurement (elapsed time = 0) was recorded. While the reaction mixture was stirred at 25 °C, the absorptivity was recorded at various time intervals until the absorbance was less than 25% of the initial reading. A plot of  $\ln(A_0/A_t)$  vs time gave a slope equal to the *pseudo*-first-order rate constant, which was converted into the overall second-order rate constant by correcting for the concentration of nucleophile. Identification of reaction products was accomplished by mixture melting points, chromatographic analyses, and spectral comparisons with authentic samples. For example, a solution of the CCMB anhydro-5,7-dimethyl-2-ethyl-1-hydroxy-3-oxopyrazolo[1,2-*a*]pyrazolium hydroxide (0.47 g, 2.4 mmol) in THF (25 mL) was treated with aniline (10.0 g, 108 mmol) for 5 days at 25 °C. After evaporation of the THF and excess aniline, chromatography (silica gel, hexane/methylene chloride/ether) afforded 3,5-dimethylpyrazole (0.21 g, 91%) as colorless needles from  $\text{EtOH}$ , mp 106–107 °C (lit.<sup>32</sup> mp 107 °C), and ethylmalonic acid dianilide (0.59 g, 86%) as colorless needles from  $\text{EtOH}/\text{H}_2\text{O}$ , mp 213–214 °C (lit.<sup>33</sup> mp 213–215 °C). Similarly, a solution of the PCCMB anhydro-1-hydroxy-3-oxo-2-phenylpyrrolo[1,2-*a*]pyridinium hydroxide (2) (0.51 g, 2.3 mmol) in THF (25 mL) was treated with morpholine (10.0 g, 1.15 mmol) for 10 days at 25 °C. The reaction mixture was separated by HPLC (silica gel, hexane/methylene chloride/ether) to obtain phenylmalonic acid dimorpholide (0.64 g, 84%) as colorless prisms from  $\text{CH}_2\text{Cl}_2/\text{Et}_2\text{O}$ , mp 175 °C (lit.<sup>25</sup> mp 175 °C), and pyridine, which was acidified with 10% dilute HCl and isolated as pyridine hydrochloride (0.26 g, 85%) as colorless prisms from ethanol, mp 82 °C (lit.<sup>34</sup> mp 82 °C).

**Acknowledgment.** We thank Dr. R. K. Kullnig, Sterling Winthrop Research Institute, for the determination of the single-crystal X-ray structure, Prof. H. Herbrandson for many helpful discussions, and IBM for the award of a Fellowship (P.M.M.). Grants from the National Science Foundation and U.S. Public Health Service for the purchase of the major equipment used in these studies are gratefully acknowledged.

**Registry No.** 1, 75526-82-8; 2, 91994-41-1; 4, 91994-35-3; 4 (7-phenyl deriv), 114505-26-9; 5, 97938-47-1; 5a, 102860-35-5; 6, 114492-26-1; 7a, 114492-27-2; 7b, 114492-42-1; 7 (2-allyl deriv), 114492-43-2; 8, 79815-57-9; 8 (demethyl deriv), 114492-46-5; 9a, 102860-36-6; 9b, 102860-37-7; 9 (X =  $\text{C}_6\text{H}_5$ , 6-chloro deriv), 114492-31-8; 9 (X =  $\text{C}_6\text{H}_5$ ), 76434-58-7; 9 (X =  $\text{C}_2\text{H}_5$ ), 76426-55-6; 9 (X = CN), 91994-39-7; 9 (X = allyl), 114492-39-6; 9 (X = isopropenyl), 114492-40-9; 9 (X =  $(\text{CH}_2)_2\text{Cl}$ ), 114492-44-3; 9 (X = CN, thioxo deriv), 91994-40-0; 10a, 114492-29-4; 11b, 114492-30-7; 11b (X =  $\text{OCH}_3$ ), 79815-65-9; 11b (Y =  $\text{NH}_2$ ), 114492-45-4; 11c, 114492-32-9; 11d, 114492-33-0; 11e, 79815-61-5; 11f, 114492-37-4; 11 (R =  $\text{C}_6\text{H}_5$ , X = Y = H), 79815-55-7; 18, 91994-36-4; 19, 114492-35-2; 20, 114492-36-3; 22, 5519-42-6; 24, 114492-38-5;  $\text{C}_6\text{H}_5\text{NH}_2$ , 62-53-3; 3,5-dimethylpyrazole, 67-51-6; ethylmalonic acid dianilide, 10256-07-2; morpholine, 110-91-8; phenylmalonic acid dimorpholide, 79815-71-7; pyridine hydrochloride, 628-13-7; anhydro-5,7-dimethyl-3-hydroxy-2-phenyl-1-(*p*-tolylsulfonilimino)pyrazolo[1,2-*a*]pyrazolium hydroxide, 91994-37-5; anhydro-3-(dicyanomethyl)-5,7-dimethyl-1-oxo-2-phenylpyrazolo[1,2-*a*]pyrazolium hydroxide, 91994-38-6; anhydro-5-hydroxy-7-oxo-6-phenyl-7*H*-imidazo[1,2-*a*]pyrido[3,2-*c*][1,4]diazepinium hydroxide, 114492-41-0.

**Supplementary Material Available:** Crystal data, atomic coordinates, and isotropic thermal parameters for anhydro-1-hydroxy-3-oxo-2-phenylpyrrolo[1,2-*a*]pyridinium hydroxide (2) (4 pages). Ordering information is given on any current masthead page.

(33) Freund, M.; Goldsmith, B. B. *Ber. Dtsch. Chem. Ges.* 1888, 21, 1245.

(34) Heilbron, I. M. *Dictionary of Organic Compounds*; Oxford University: Oxford, 1938; Vol. III.